Electronic Supplementary Information

- **Figure S1.** IR spectrum of [Sb(Bha$_{-1H}$)$_2$Cl].
- **Figure S2.** ^{1}H NMR spectrum of [Sb(Bha$_{-1H}$)$_2$Cl].
- **Figure S3.** ^{1}H NMR spectrum of Bha.
- **Figure S4.** ^{1}H NMR spectra of [Sb(Bha$_{-1H}$)$_2$Cl] over time, 0-72 h.
- **Figure S5.** ^{13}C NMR spectrum of [Sb(Bha$_{-1H}$)$_2$Cl].
- **Figure S6.** Mass spectrum of [Sb(Bha$_{-1H}$)$_2$Cl].
- **Figure S7.** IR spectrum of [SbCl$_2$(2-pyha$_{-1H}$)].
- **Figure S8.** ^{1}H NMR spectrum of [SbCl$_2$(2-pyha$_{-1H}$)].
- **Figure S9.** ^{1}H NMR spectrum of 2-pyha.
- **Figure S10.** ^{1}H NMR spectra of [SbCl$_2$(2-pyha$_{-1H}$)] over time, 0-72 h.
- **Figure S11.** ^{13}C NMR spectrum of [Sb$_2$(μ-Cl)$_2$(Cl)$_2$(2-pyha$_{-1H}$)$_2$].
- **Figure S12.** Mass spectrum of [Sb$_2$(μ-Cl)$_2$(Cl)$_2$(2-pyha$_{-1H}$)$_2$].
- **Figure S13.** IR spectrum of [Sb(2-NH$_2$-pha$_{-1H}$)(2-NH$_3$-pha$_{-1H}$)]Cl$_2$.
- **Figure S14.** ^{1}H NMR spectrum of [Sb(2-NH$_2$-pha$_{-1H}$)(2-NH$_3$-pha$_{-1H}$)]Cl$_2$.
- **Figure S15.** ^{1}H NMR spectrum 2-NH$_2$-pha.
- **Figure S16.** ^{1}H NMR spectra of [Sb(2-NH$_2$-pha$_{-1H}$)(2-NH$_3$-pha$_{-1H}$)]Cl$_2$ over time, 0-72 h.
- **Figure S17.** ^{13}C NMR spectrum of [Sb(2-NH$_2$-pha$_{-1H}$)(2-NH$_3$-pha$_{-1H}$)]Cl$_2$.
- **Figure S18.** Mass spectrum of [Sb(2-NH$_2$-pha$_{-1H}$)(2-NH$_3$-pha$_{-1H}$)]Cl$_2$.
- **Figure S19.** IR spectrum of [SbCl(Sha$_{-1H}$)$_2$].
- **Figure S20.** 1H NMR spectrum of [SbCl(Sha$_{-1H}$)$_2$].
- **Figure S21.** 1H NMR spectrum of Sha.
- **Figure S22.** ^{1}H NMR [SbCl(Sha$_{-1H}$)$_2$] (red) overlayed with Sha (green).
- **Figure S23.** ^{1}H NMR spectra of [SbCl(Sha$_{-1H}$)$_2$] over time, 0-72 h.
- **Figure S24.** ^{13}C NMR spectrum of [SbCl(Sha$_{-1H}$)$_2$].
- **Figure S25.** Mass spectrum of [SbCl(Sha$_{-1H}$)$_2$].
- **Figure S26.** IR spectrum of 5.
- **Figure S27.** ^{1}H NMR spectrum of 5.
- **Figure S28.** ^{1}H NMR spectrum of SAHA.
- **Figure S29.** ^{13}C NMR spectrum of 5.
- **Figure S30.** Mass spectrum of 5.
- **Figure S31.** IR spectrum of [Sb(SAHA$_{-1H}$)(SAHA$_{-2H}$)].
- **Figure S32.** ^{1}H NMR spectrum of [Sb(SAHA$_{-1H}$)(SAHA$_{-2H}$)].
- **Figure S33.** ^{1}H NMR [Sb(SAHA$_{-1H}$)(SAHA$_{-2H}$)] (red) overlayed with SAHA (green).
- **Figure S34.** ^{1}H NMR spectra of [Sb(SAHA$_{-1H}$)(SAHA$_{-2H}$)] over time, 0-72 h.
- **Figure S35.** ^{13}C NMR spectrum of [Sb(SAHA$_{-1H}$)(SAHA$_{-2H}$)].
- **Figure S36.** Mass spectrum of [Sb(SAHA$_{-1H}$)(SAHA$_{-2H}$)].
- **Figure S37.** Packing diagram of dimeric **1** viewed normal to the b-axis showing the hydrogen bonding network.

- **Figure S38.** Hydrogen bonding pattern for **1** viewed normal to the a-axis.
- **Figure S39.** Packing diagram of the major disordered moiety of **2** showing the dimers as viewed normal to (011).
- **Figure S40:** Effects of compounds on the proliferative rate of *L. amazonensis* promastigotes.
- **Figure S41.** Effects of compounds on the proliferative rate of *L. chagasi* promastigotes.
- **Figure S42:** Effects of compounds on morphology of *L. chagasi* promastigotes.
- **Figure S43.** Promastigote forms of *L. amazonensis* (A) and *L. chagasi* (B) cell granularity (SSC) analyzed by flow cytometry post treatment.

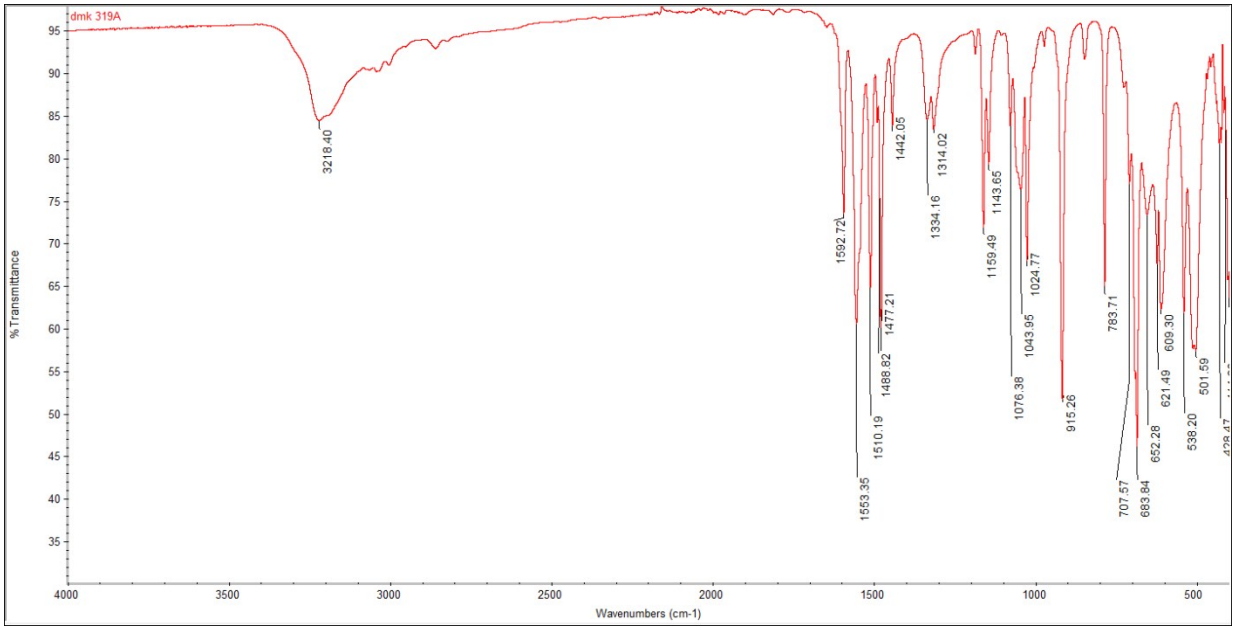

Figure S1. IR spectrum of [Sb(Bha$_{-1H}$)$_2$Cl].

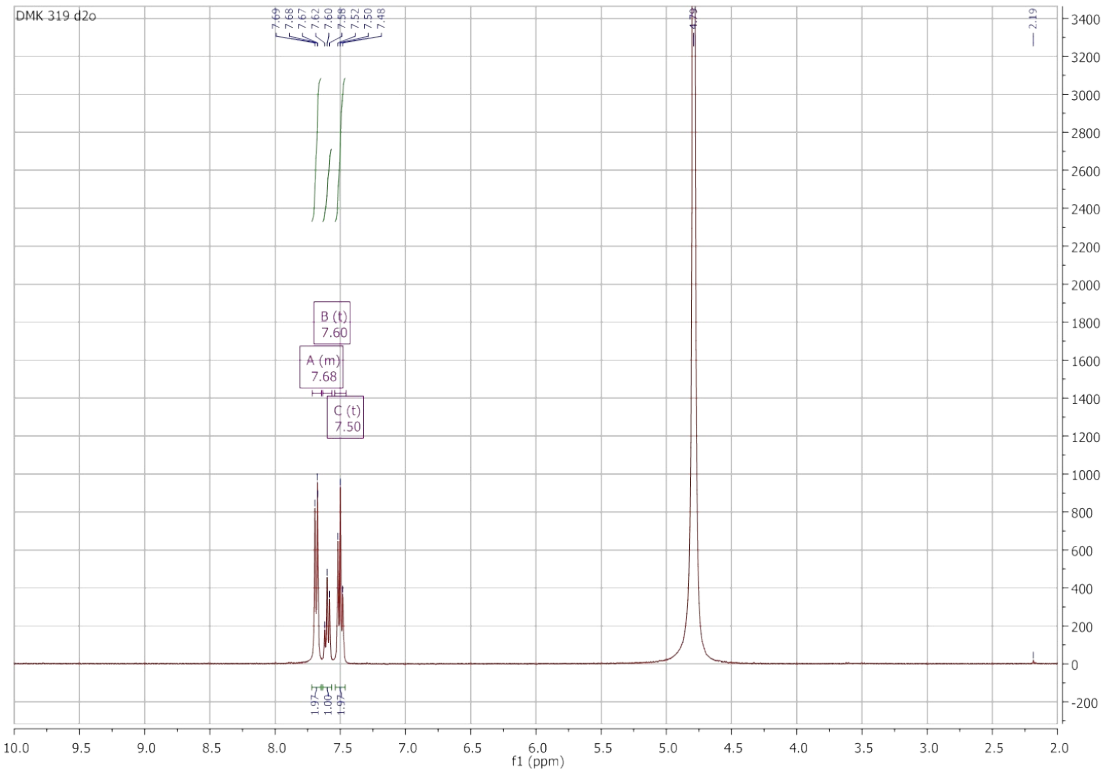

Figure S2. ^{1}H NMR spectrum of [Sb(Bha$_{-1H}$)$_2$Cl].

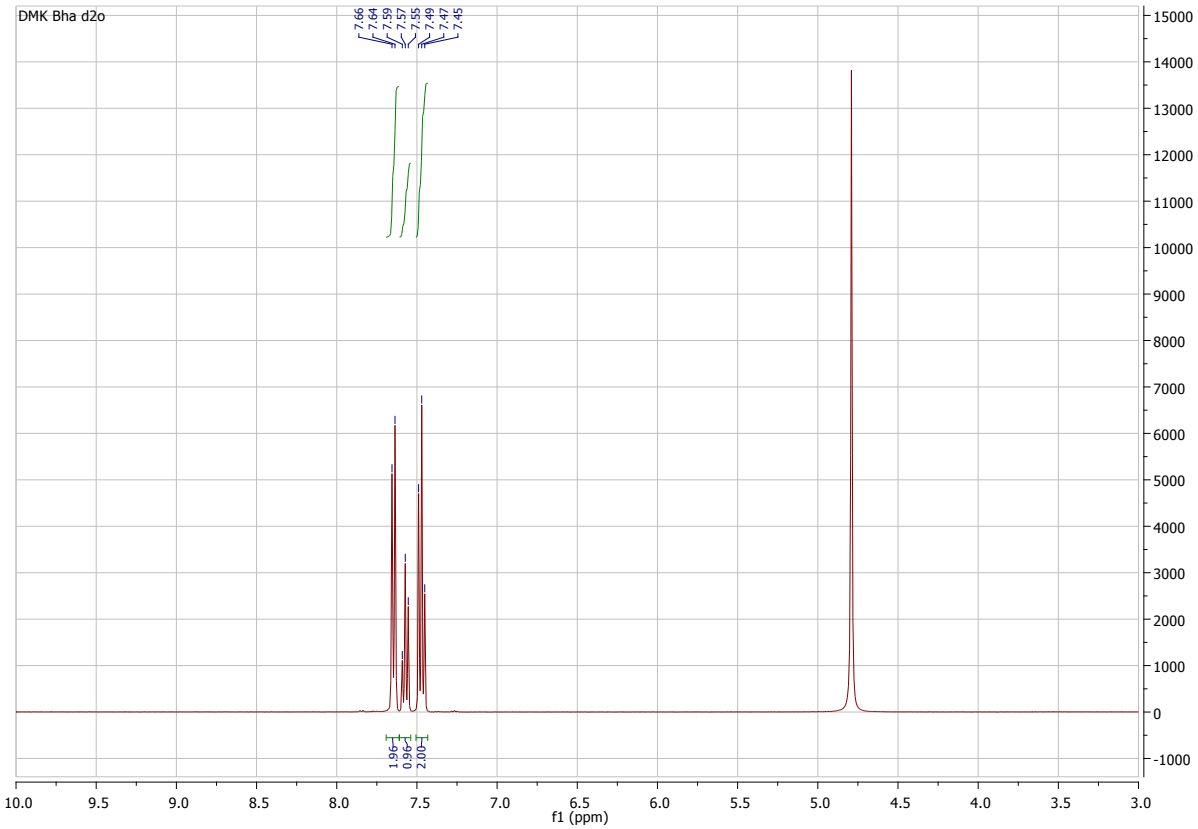

Figure S3. ^{1}H NMR spectrum of Bha.

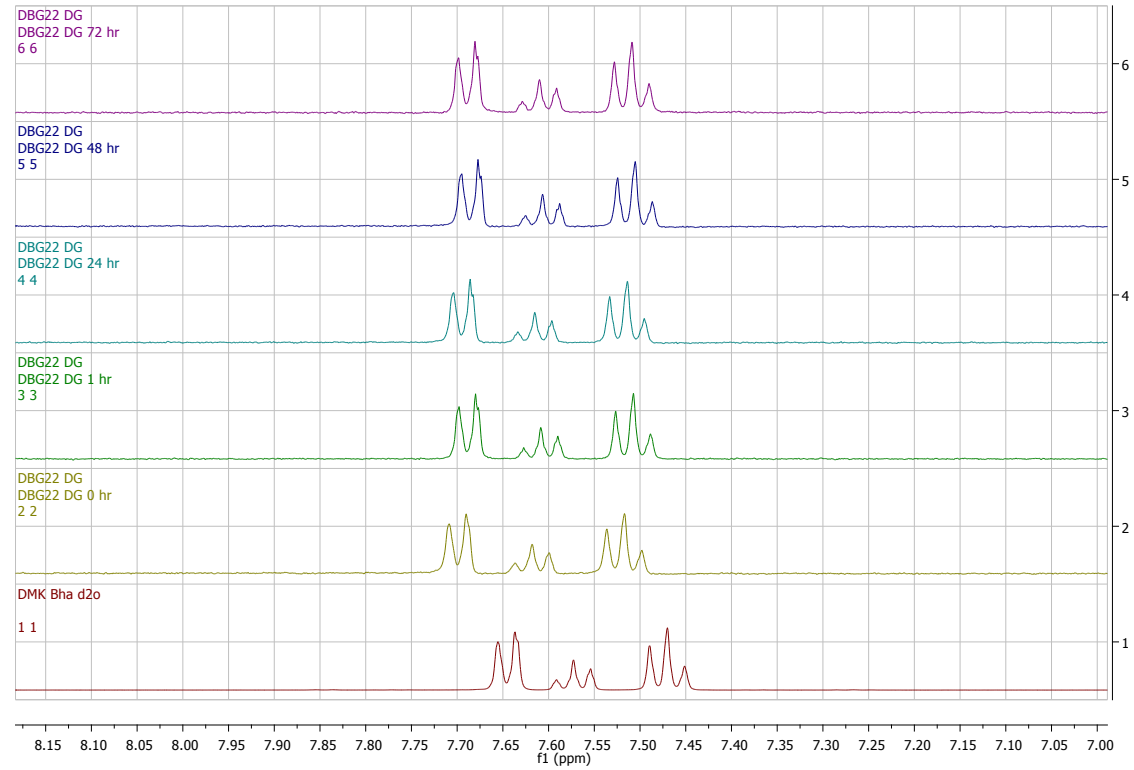

Figure S4. ^{1}H NMR spectra (D_2O) of Bha (bottom) and [$Sb(Bha_{-1H})_2Cl$] over time, 0-72 h.

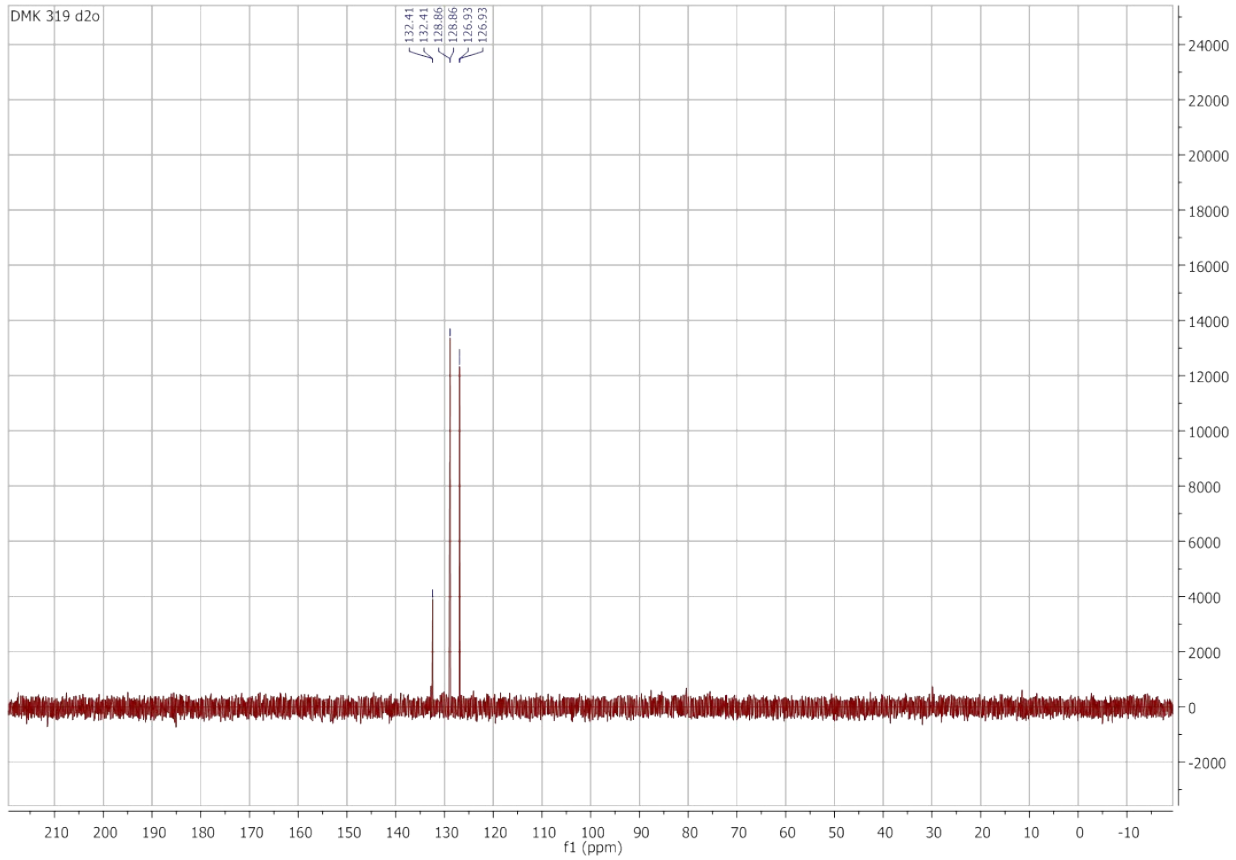

Figure S5. ^{13}C NMR spectrum of [Sb(Bha$_{-1H}$)$_2$Cl].

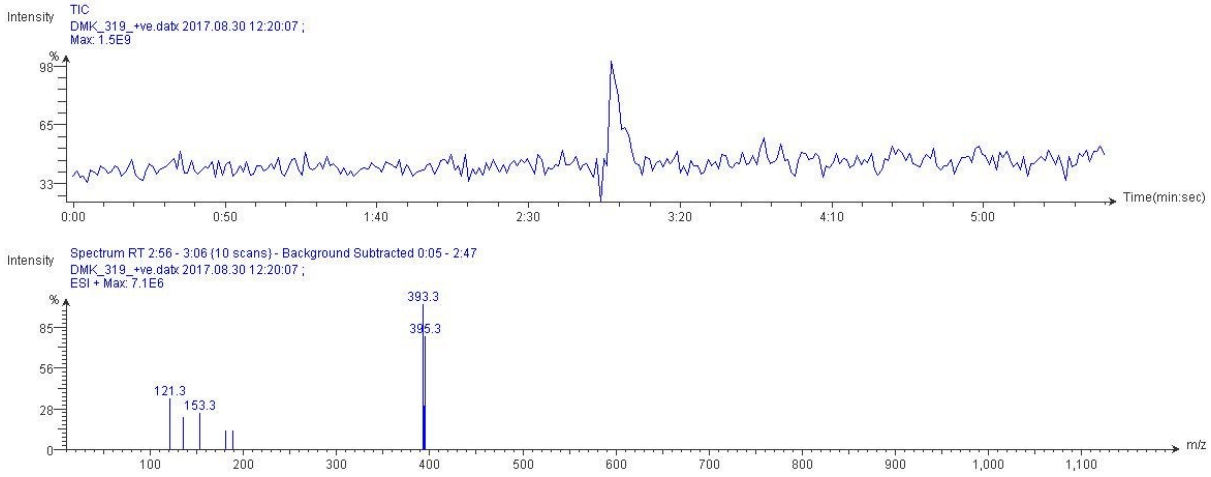

Figure S6. Mass spectrum of [Sb(Bha$_{-1H}$)$_2$Cl].

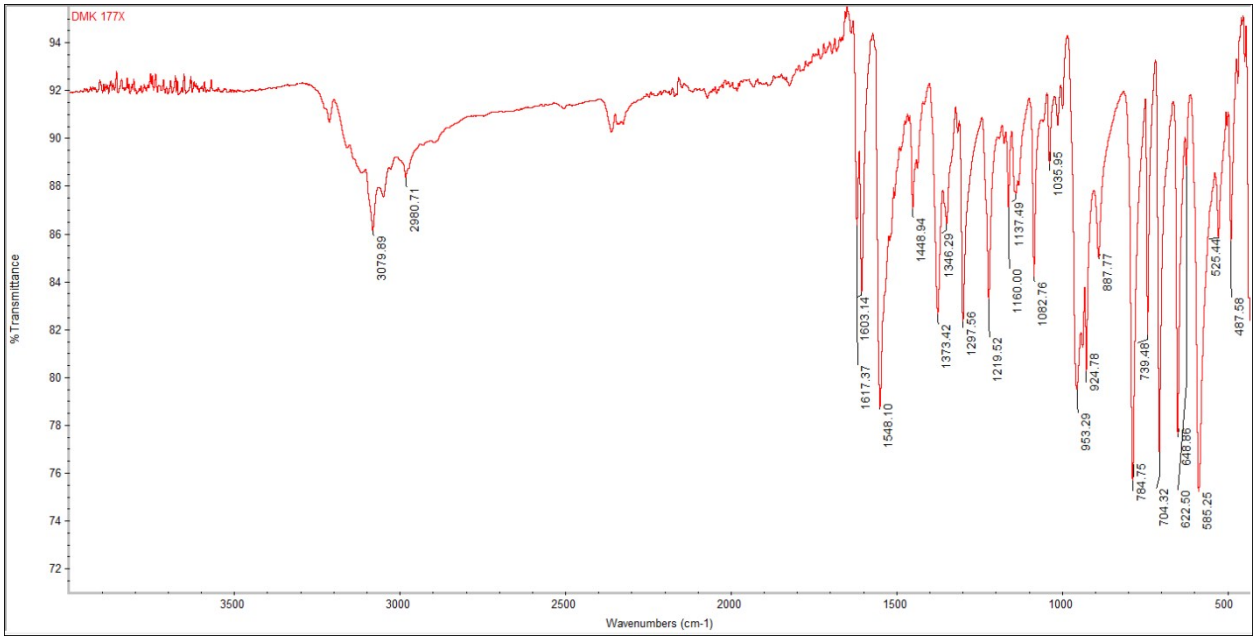

Figure S7. IR spectrum of [$SbCl_2$(2-pyha$_{-1H}$)].

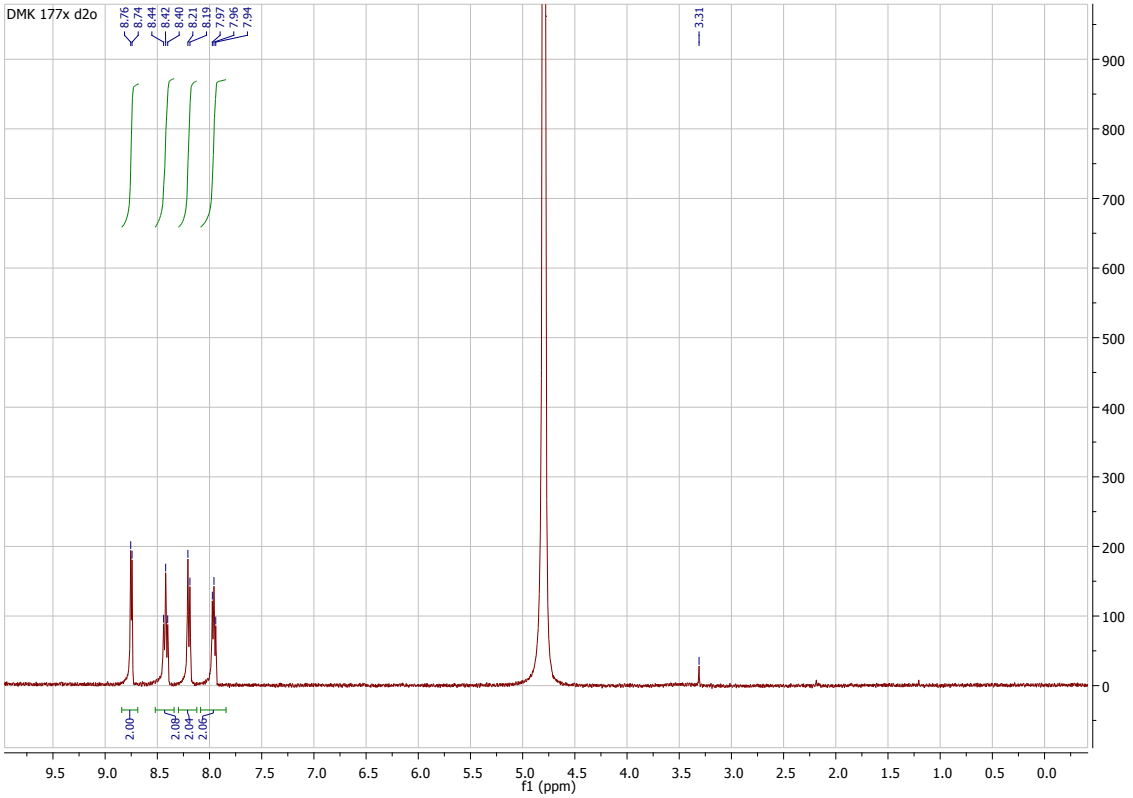

Figure S8. ^{1}H NMR spectrum of [$SbCl_2$(2-pyha$_{-1H}$)].

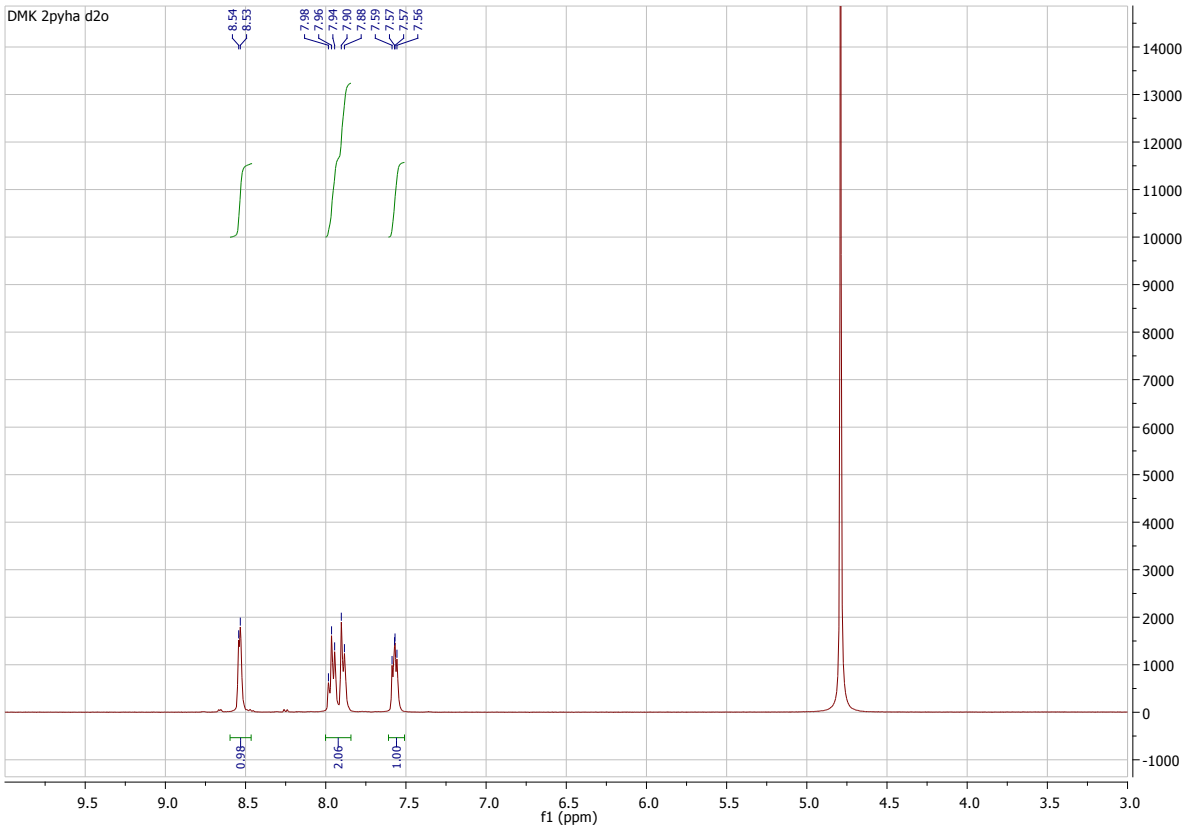

Figure S9. ^{1}H NMR spectrum of 2-pyha.

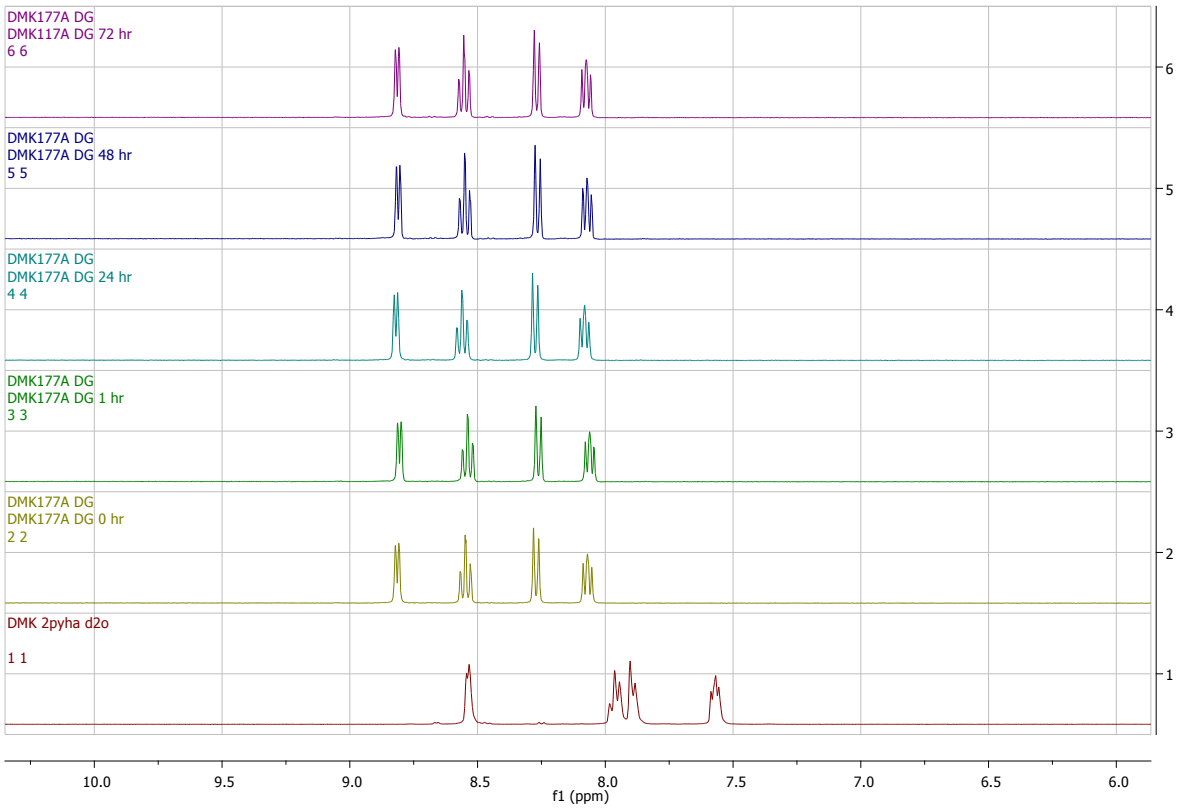

Figure S10. ^{1}H NMR spectra (D_2O) of 2-pyha (bottom) and [$SbCl_2$(2-pyha$_{-1H}$)] over time, 0-72 h.

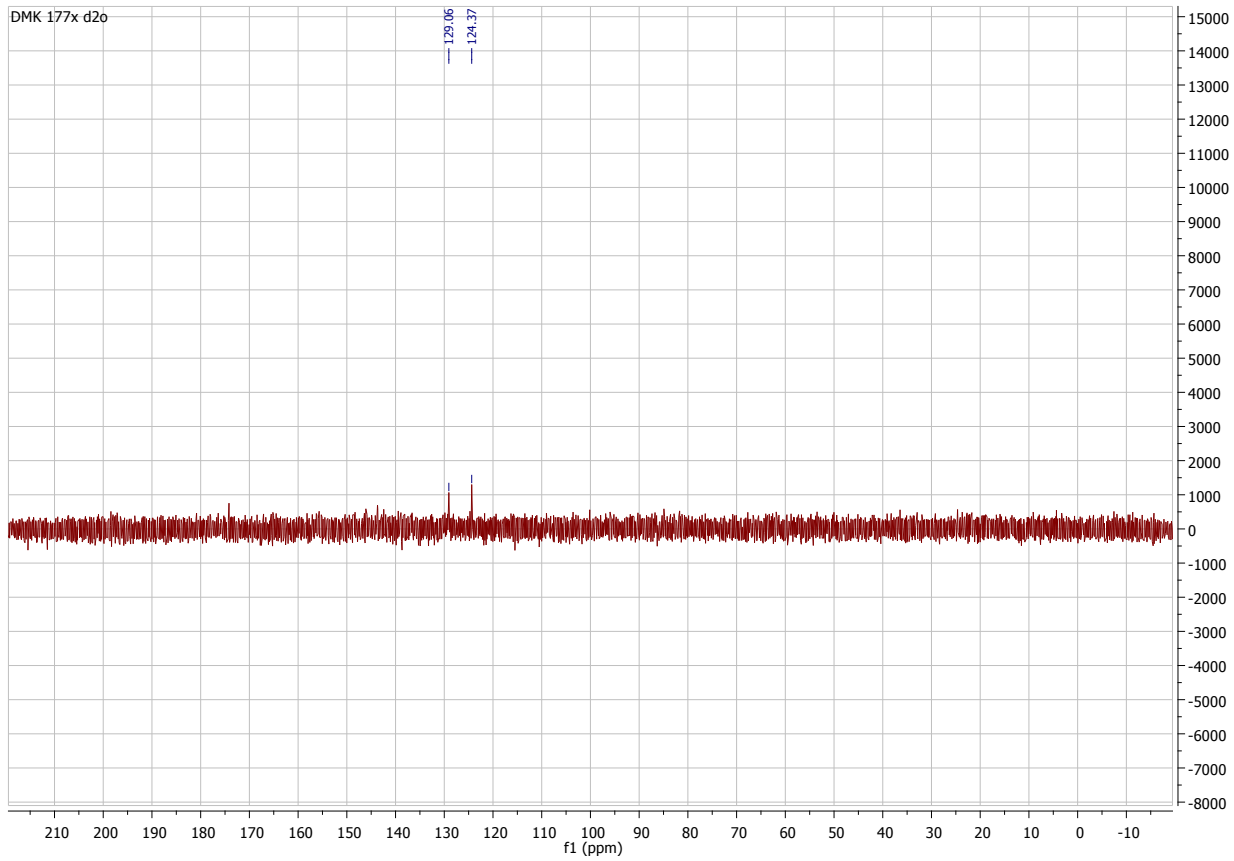

Figure S11. ^{13}C NMR spectrum of [$SbCl_2$(2-pyha$_{-1H}$)].

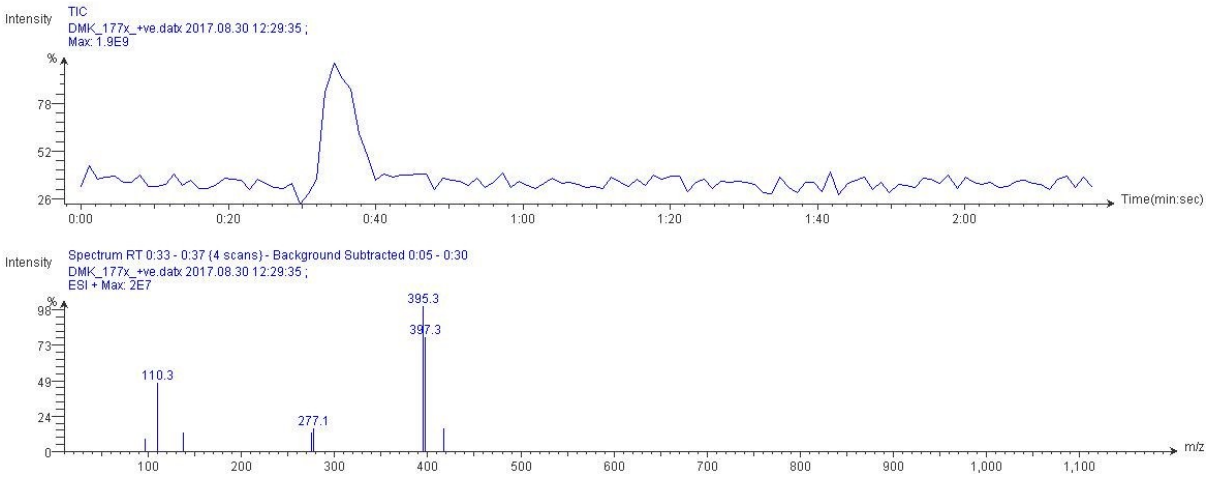

Figure S12. Mass spectrum of [$SbCl_2$(2-pyha$_{-1H}$)].

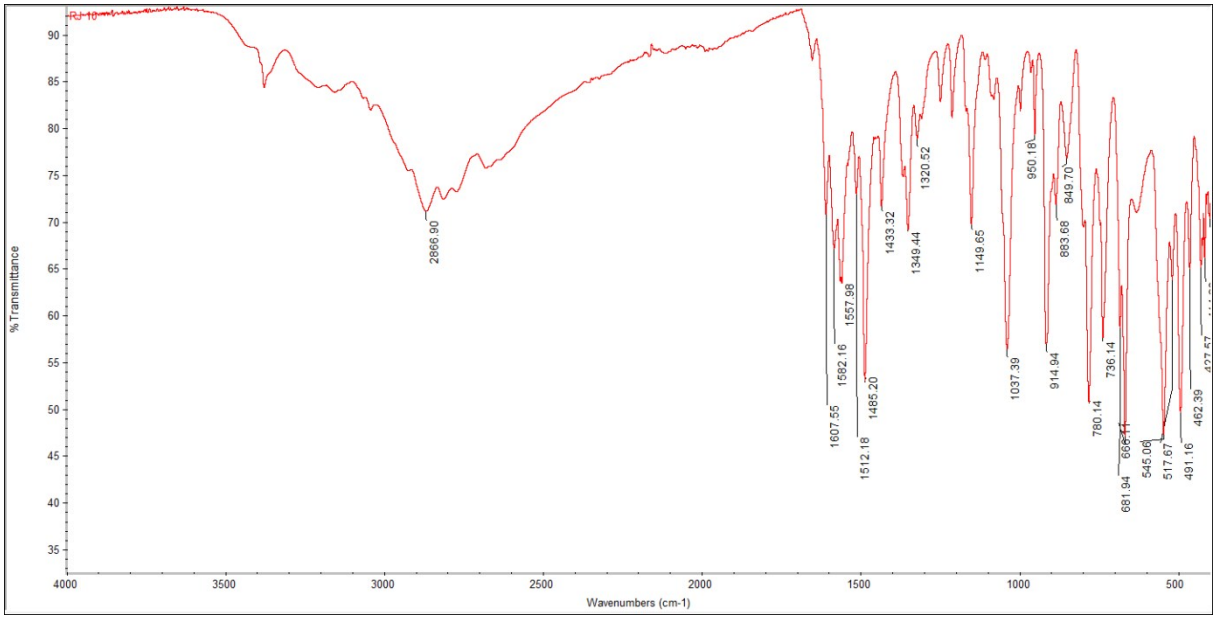

Figure S13. IR spectrum of [Sb(2-NH_2-pha$_{-1H}$)(2-NH_3-pha$_{-1H}$)]Cl_2.

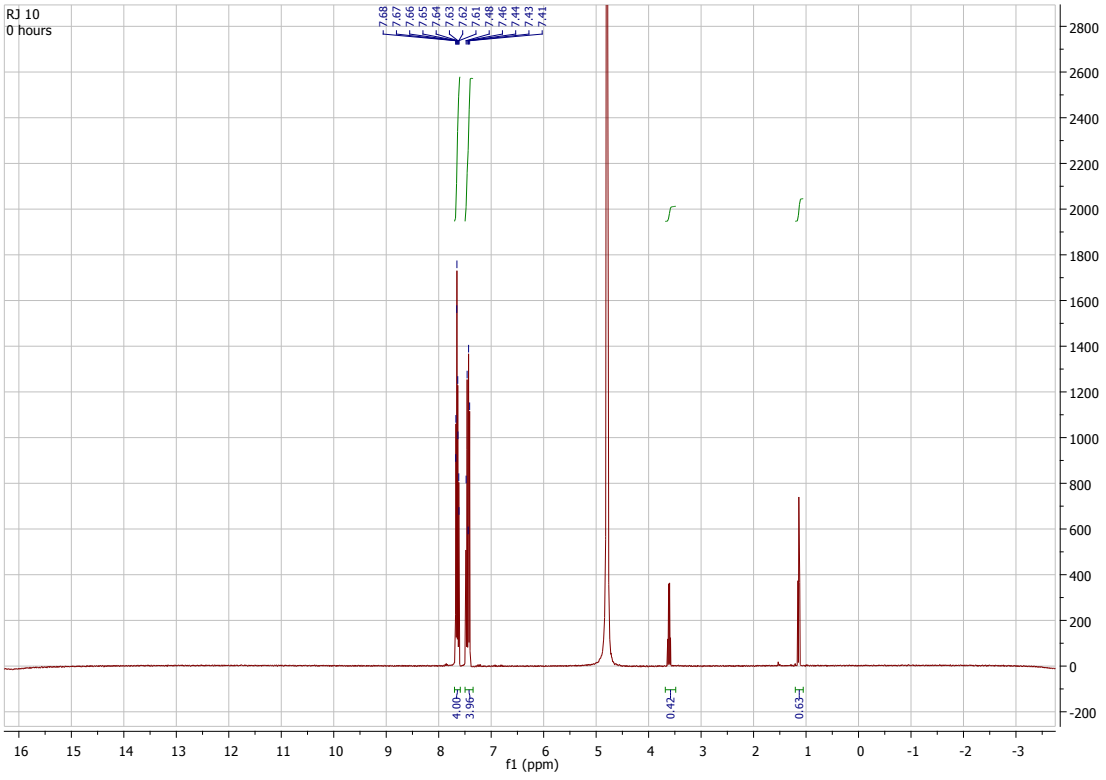

Figure S14. ^{1}H NMR spectrum of [Sb(2-NH_2-pha$_{-1H}$)(2-NH_3-pha$_{-1H}$)]Cl_2.

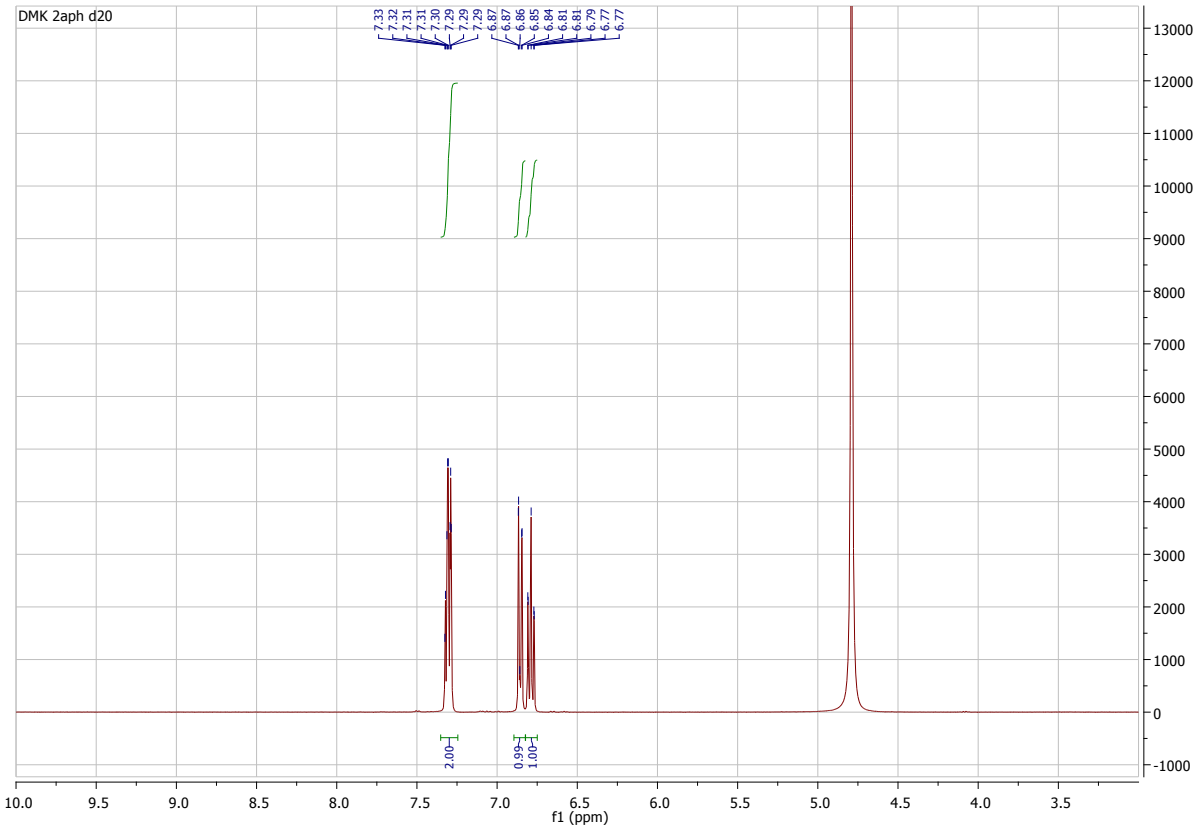

Figure S15. ^{1}H NMR spectrum 2-NH_2-pha.

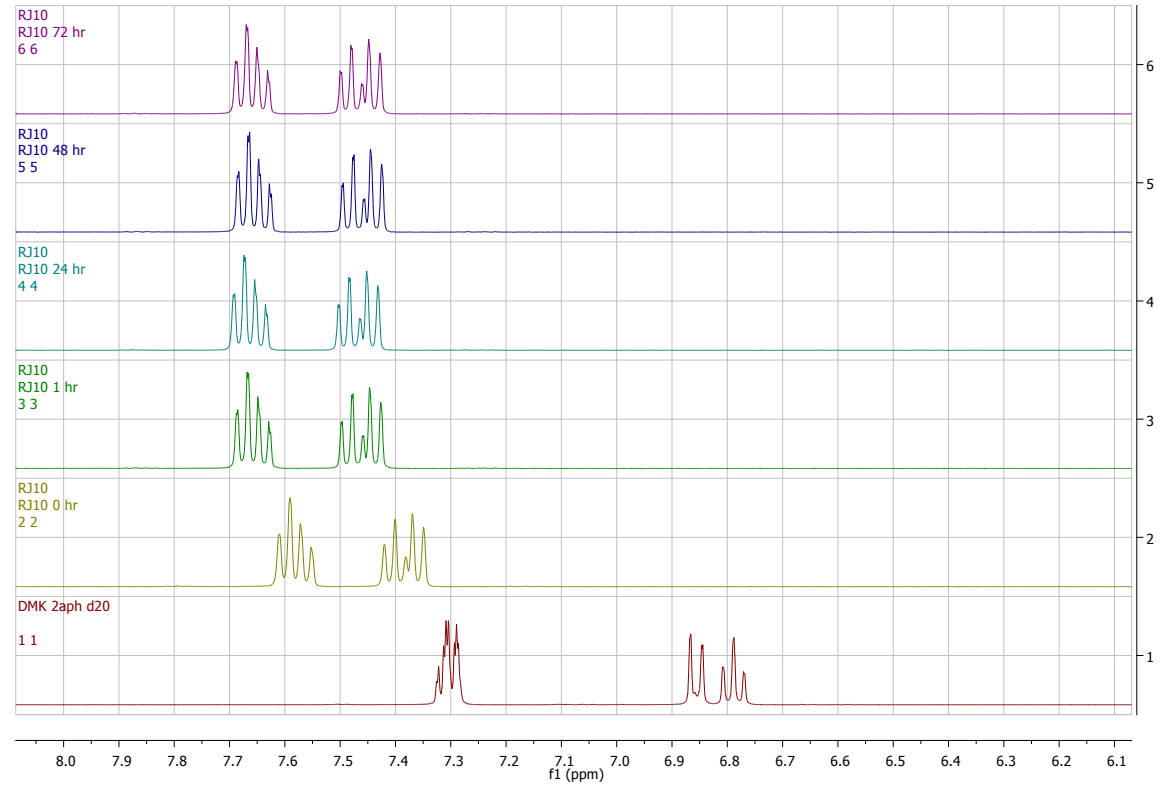

Figure S16. ^{1}H NMR spectra (D_2O) of 2-NH_2-pha$_{-1H}$ (bottom) and [Sb(2-NH_2-pha$_{-1H}$)(2-NH_3-pha$_{-1H}$)]Cl_2 over time, 0-72 h.

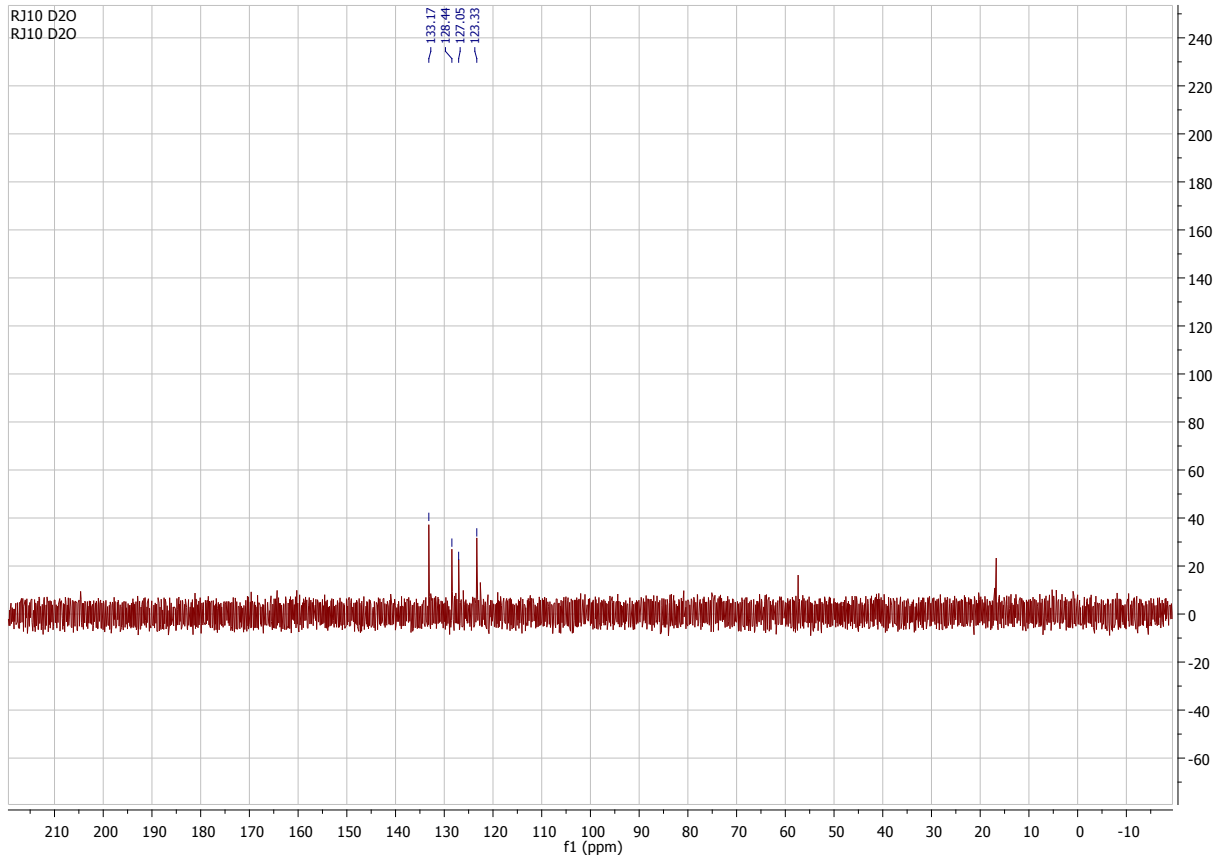

Figure S17. ^{13}C NMR spectrum of [Sb(2-NH_2-pha$_{-1H}$)(2-NH_3-pha$_{-1H}$)]Cl_2.

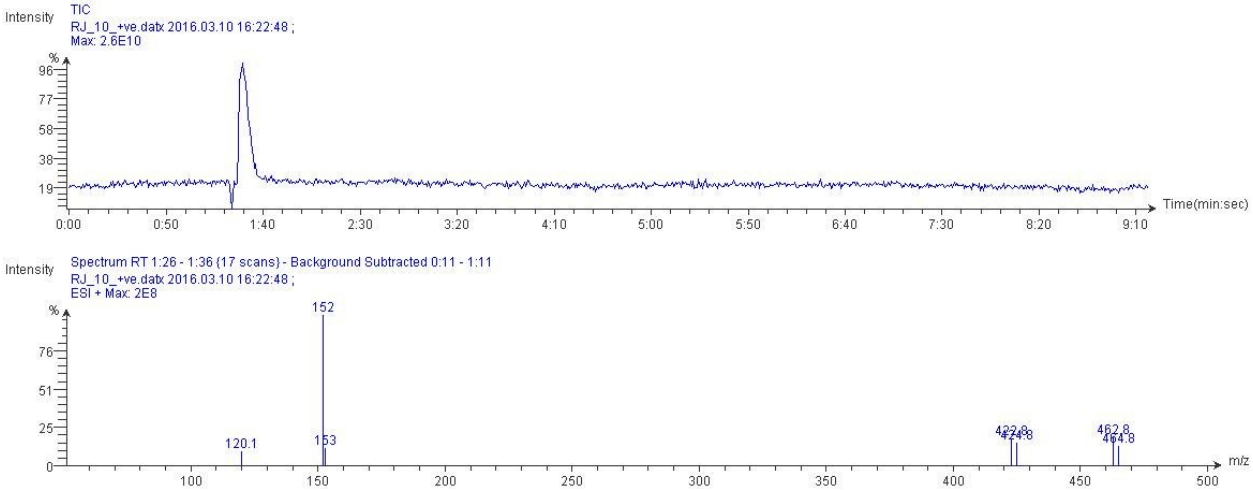

Figure S18. Mass spectrum of [Sb(2-NH_2-pha$_{-1H}$)(2-NH_3-pha$_{-1H}$)]Cl_2.

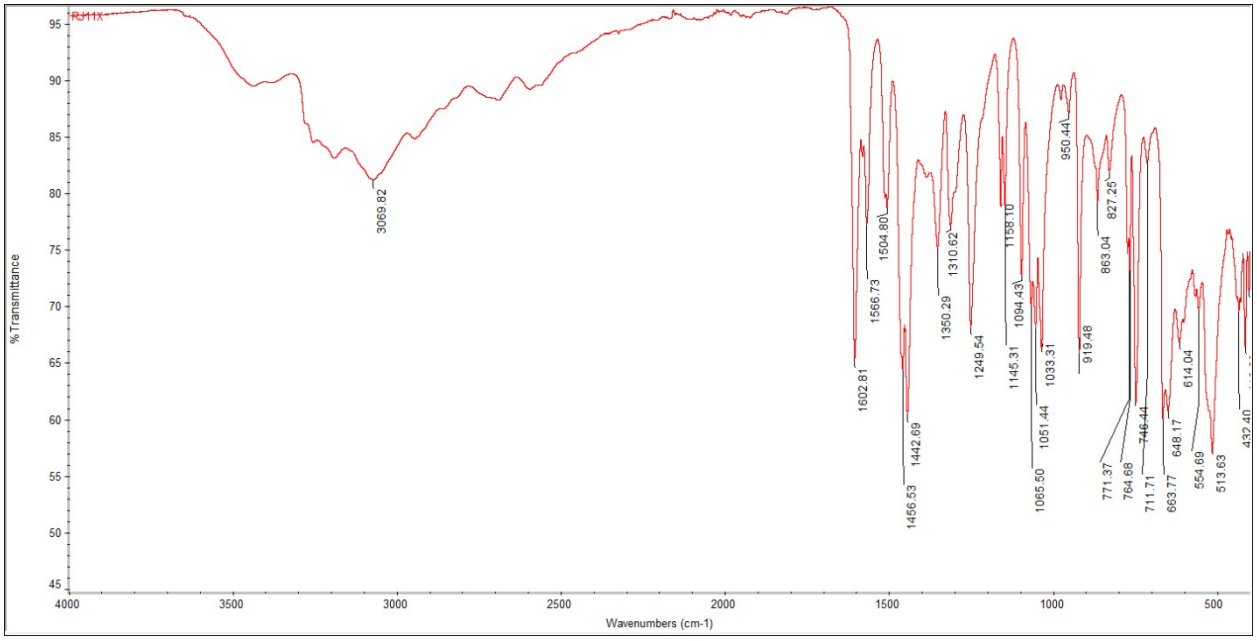

Figure S19. IR spectrum of [SbCl(Sha$_{-1H}$)$_2$].

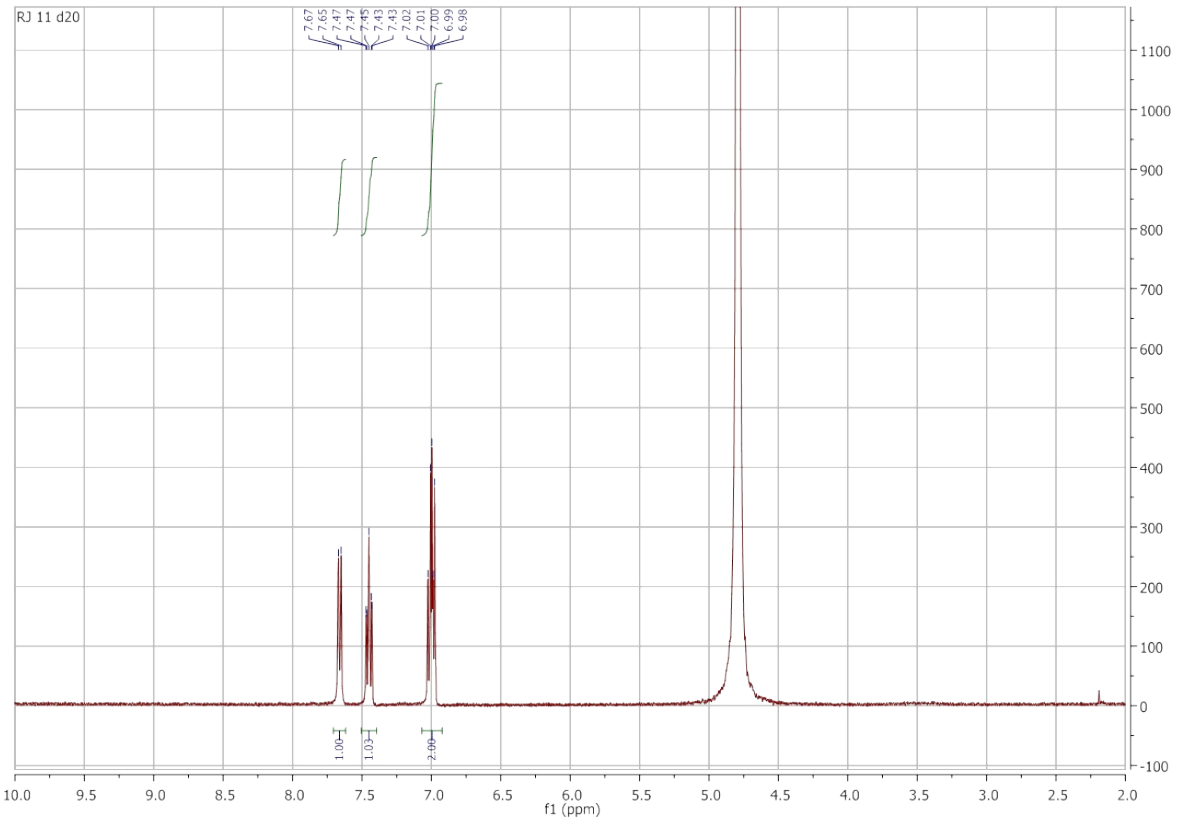

Figure S20. ^{1}H NMR spectrum of [SbCl(Sha$_{-1H}$)$_2$].

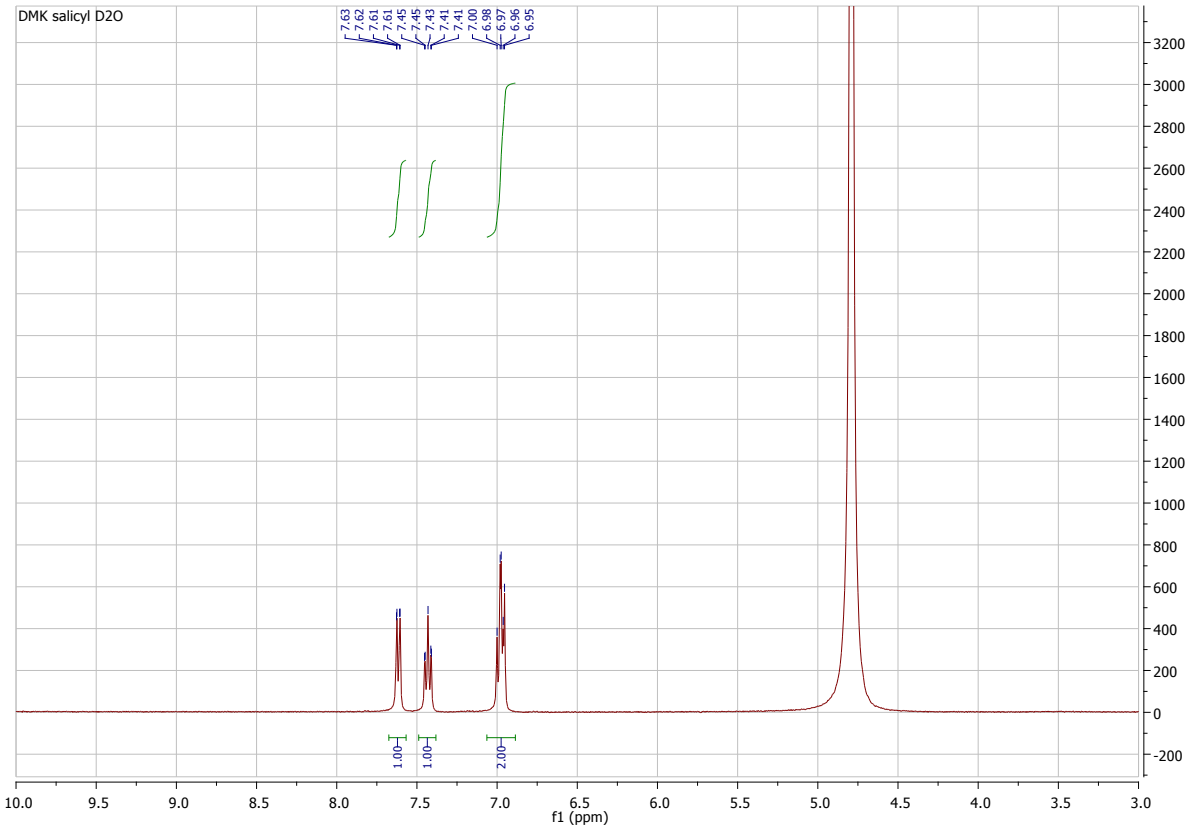

Figure S21. 1H NMR spectrum of Sha.

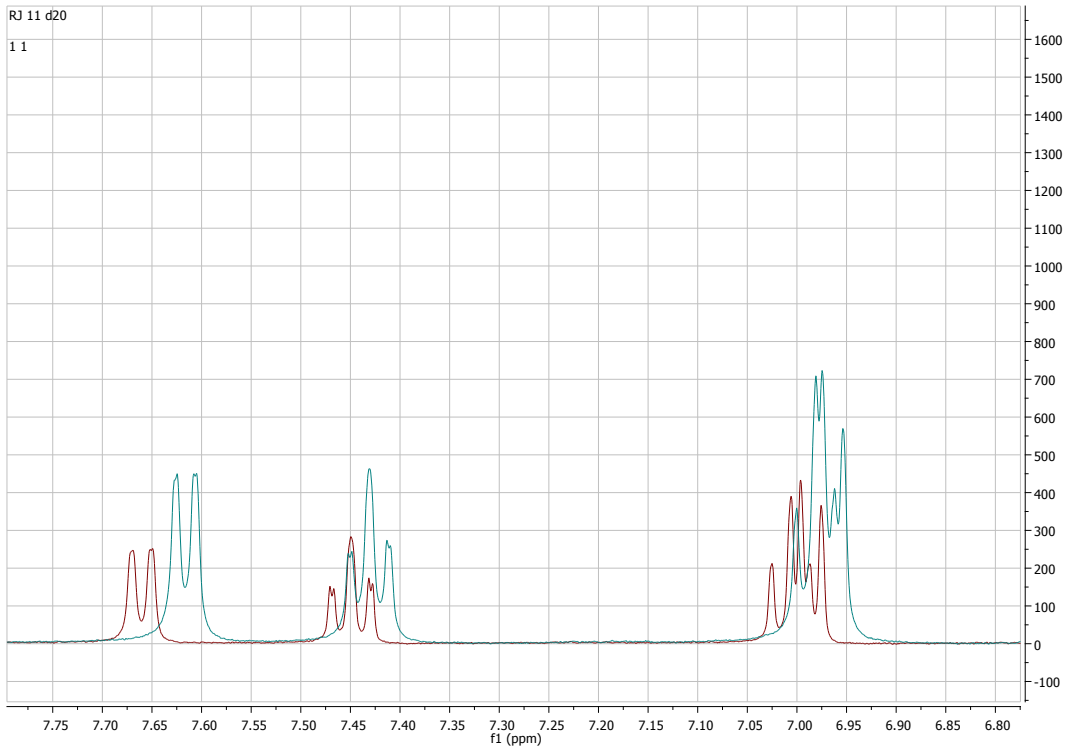

Figure S22. ^{1}H NMR [SbCl(Sha$_{-1H}$)$_2$] (red) overlayed with Sha (green).

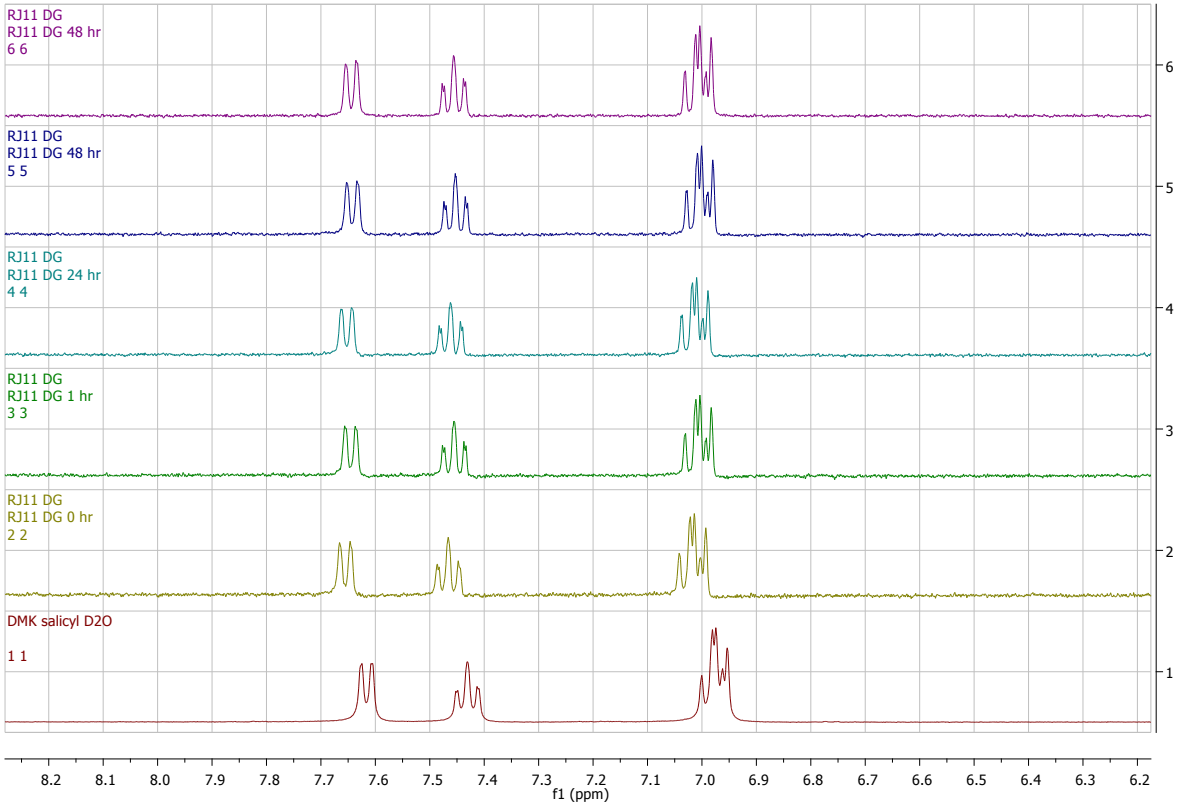

Figure S23. ^{1}H NMR spectra of Sha (bottom) and [SbCl(Sha$_{-1H}$)$_2$] over time, 0-72 h.

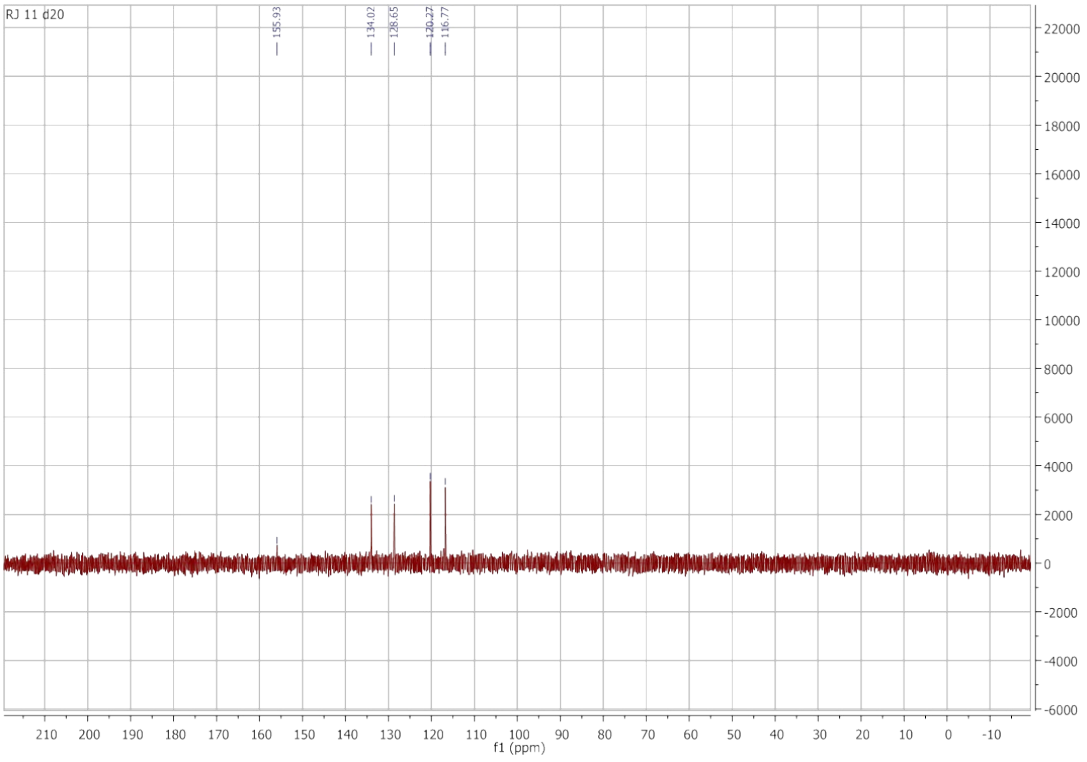

Figure S24. ^{13}C NMR spectrum of [SbCl(Sha$_{-1H}$)$_2$].

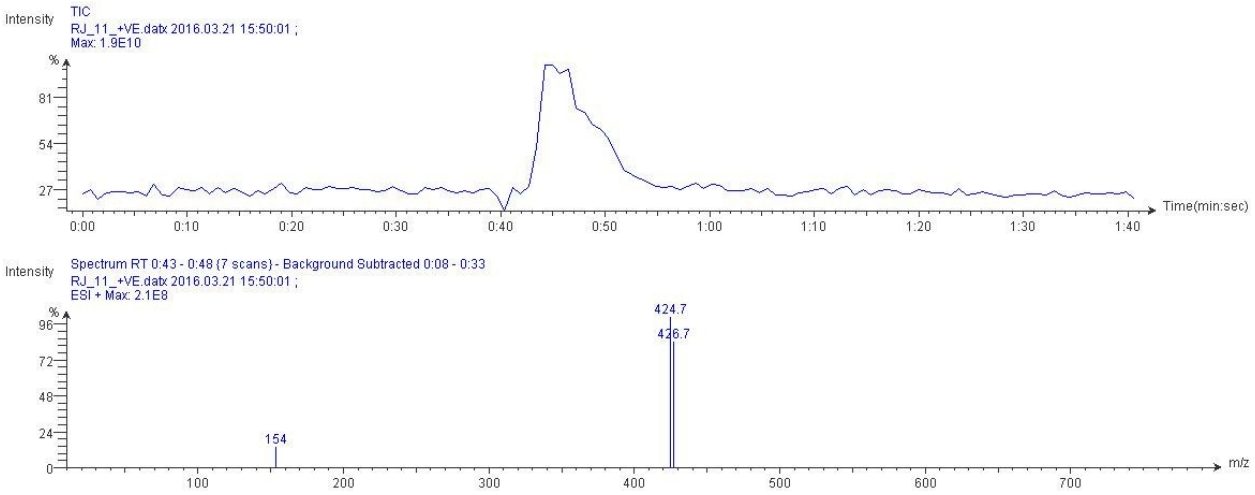

Figure S25. Mass spectrum of $[SbCl(Sha_{-1H})_2]$.

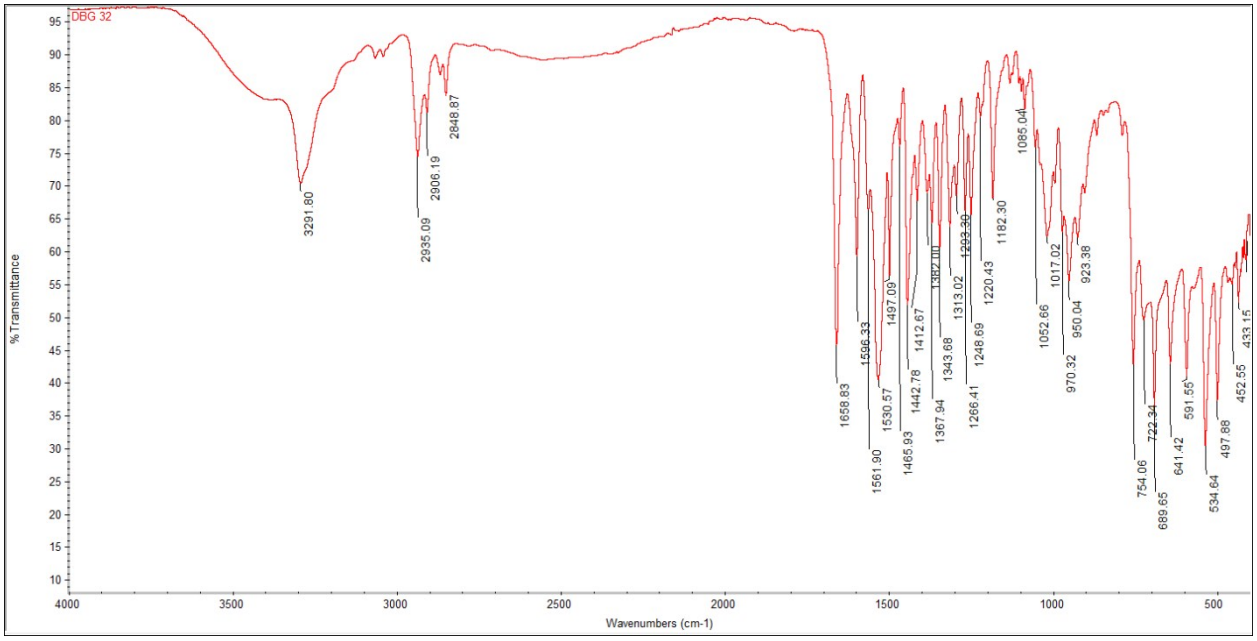

Figure S26 IR spectrum of 5.

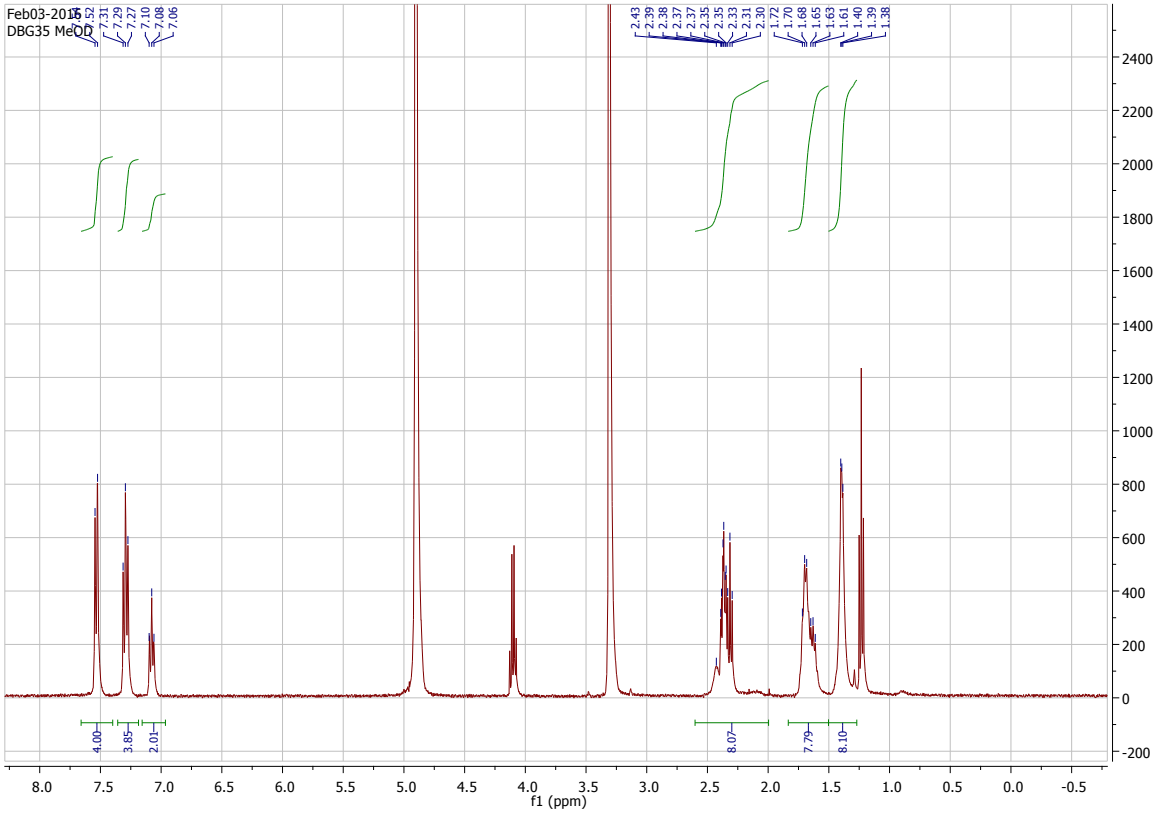

Figure S27. ^{1}H NMR spectrum of 5.

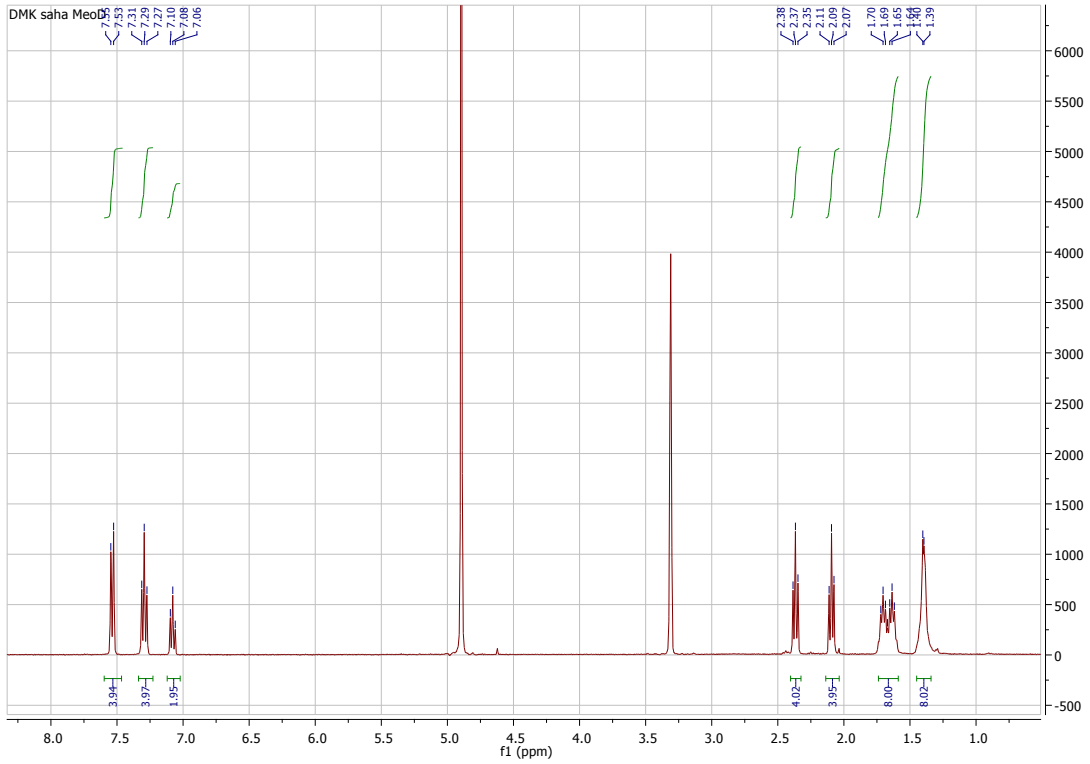

Figure S28. ^{1}H NMR spectrum of SAHA.

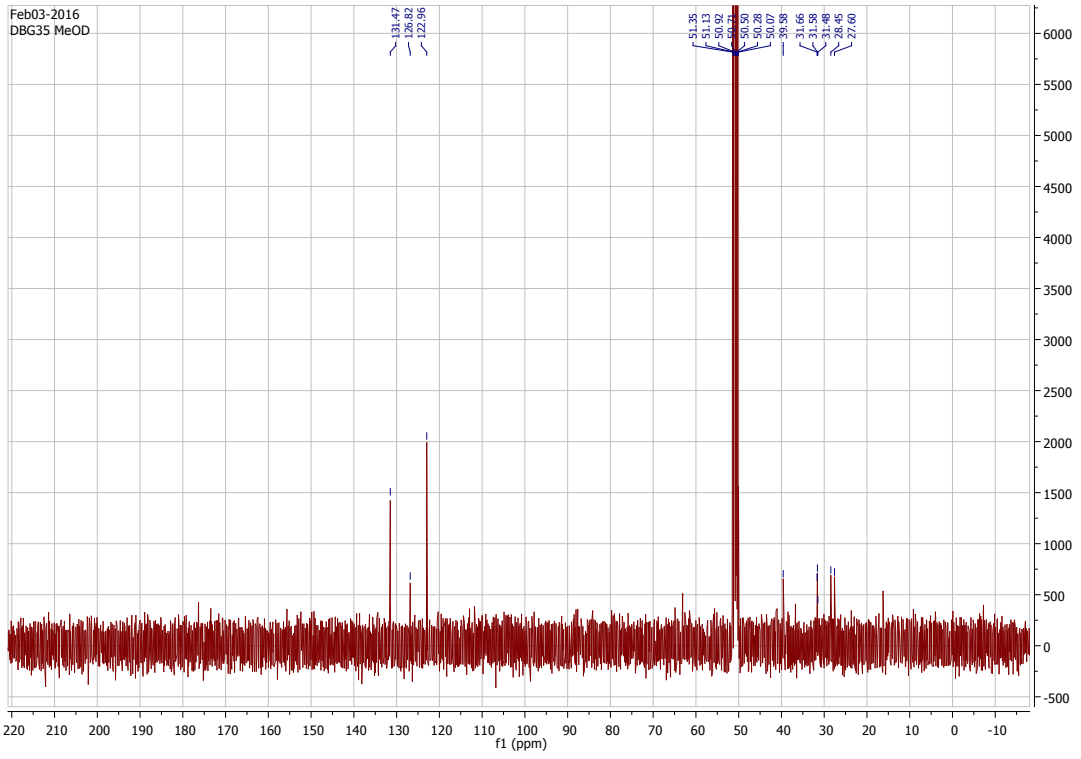

Figure S29. ^{13}C NMR spectrum of 5.

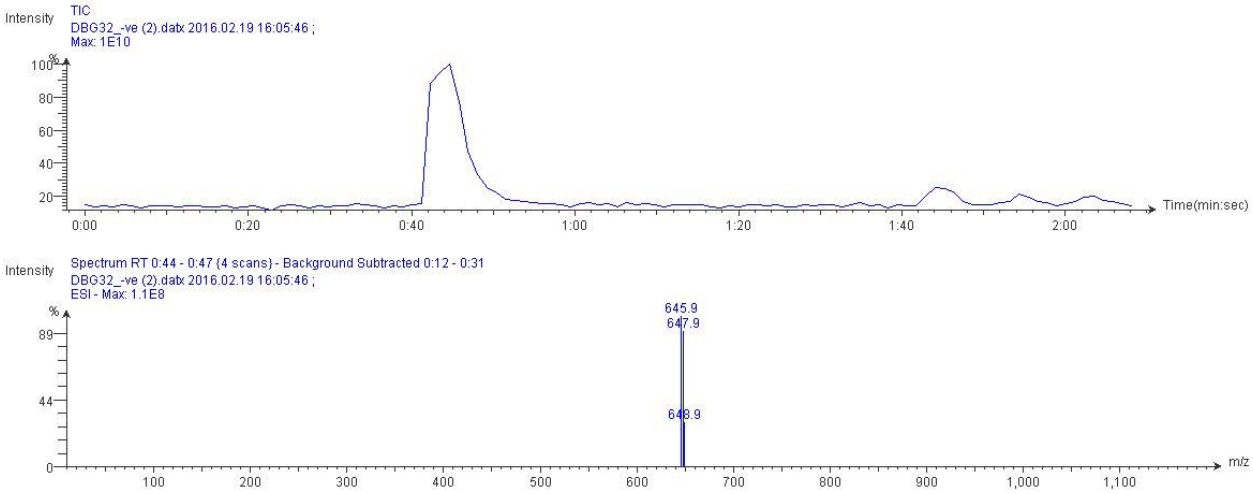

Figure S30. Mass spectrum of 5.

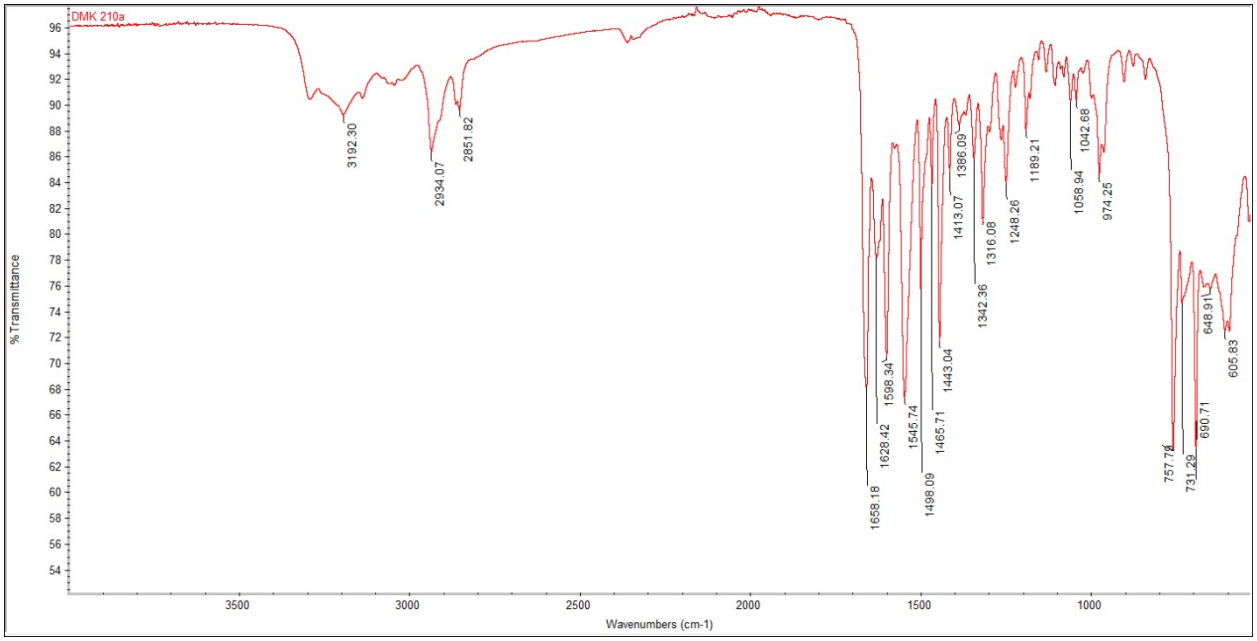

Figure S31. IR spectrum of [Sb(SAHA$_{-1H}$)(SAHA$_{-2H}$)].

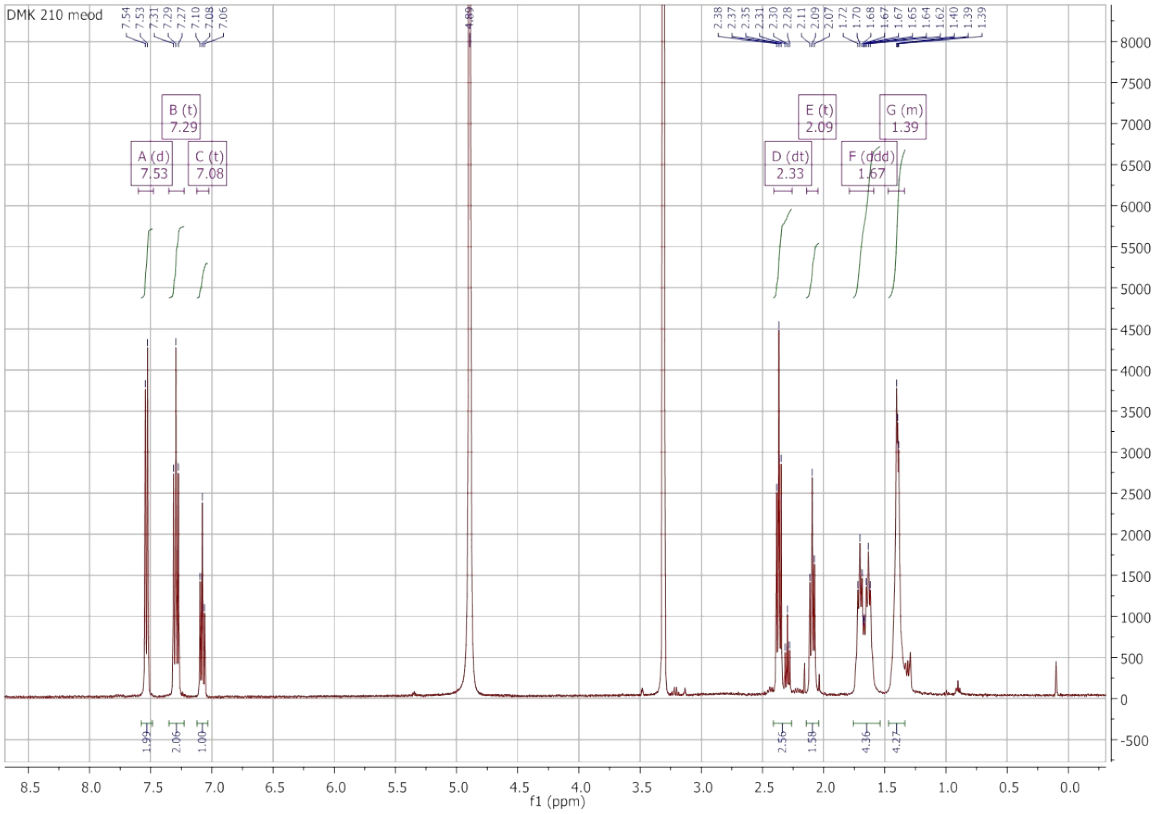

Figure S32. ^{1}H NMR spectrum of [Sb(SAHA$_{-1H}$)(SAHA$_{-2H}$)].

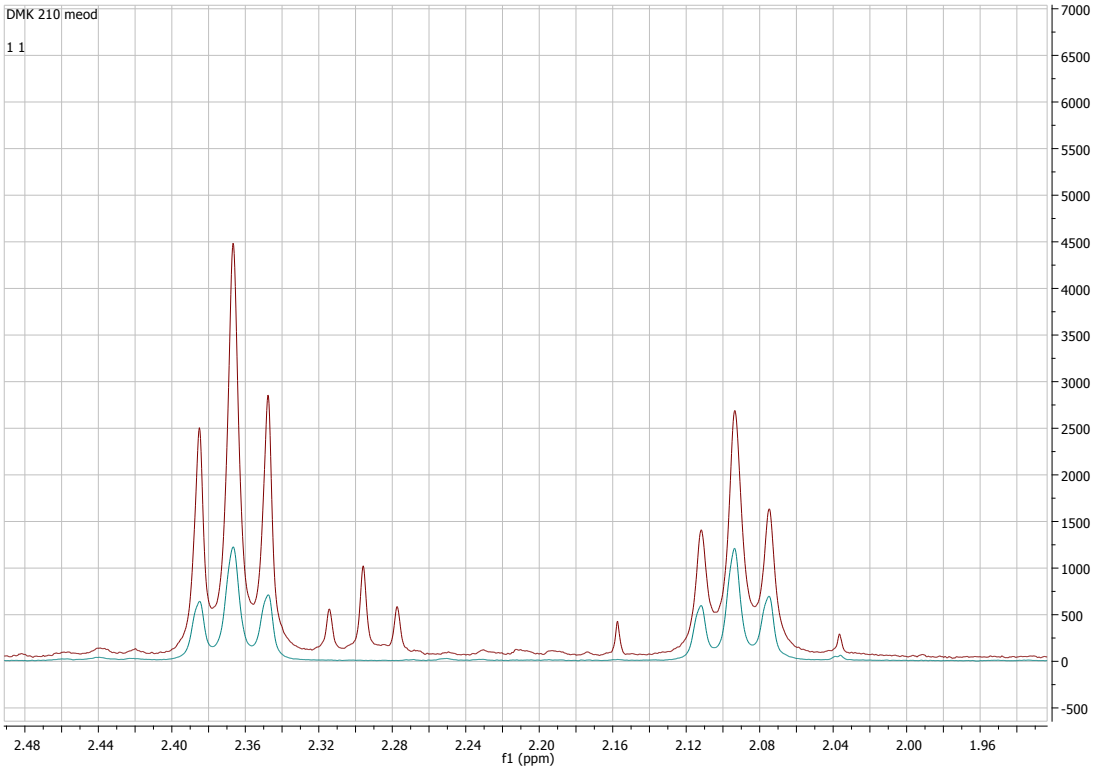

Figure S33. ^{1}H NMR spectrum [Sb(SAHA$_{-1H}$)(SAHA$_{-2H}$)] (red) overlayed with SAHA (green).

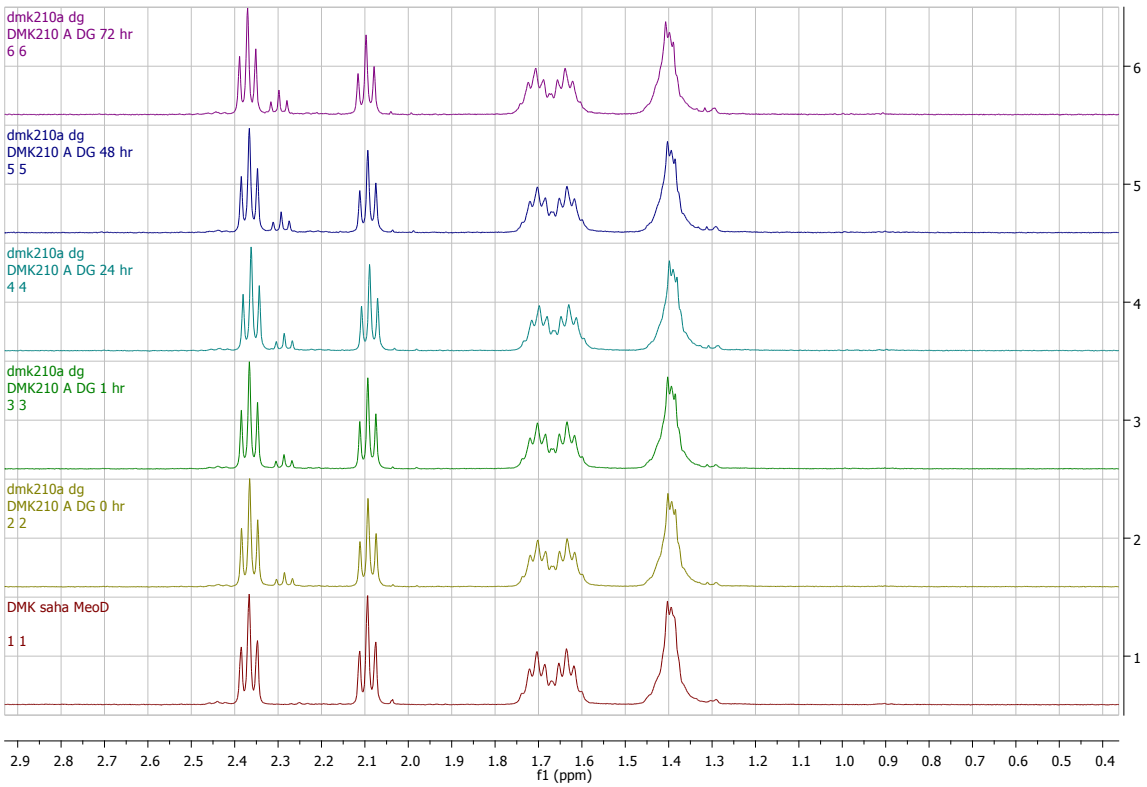

Figure S34. ^{1}H NMR spectra (CD_3OD) of SAHA bottom and [Sb(SAHA$_{-1H}$)(SAHA$_{-2H}$)] over time, 0-72 h.

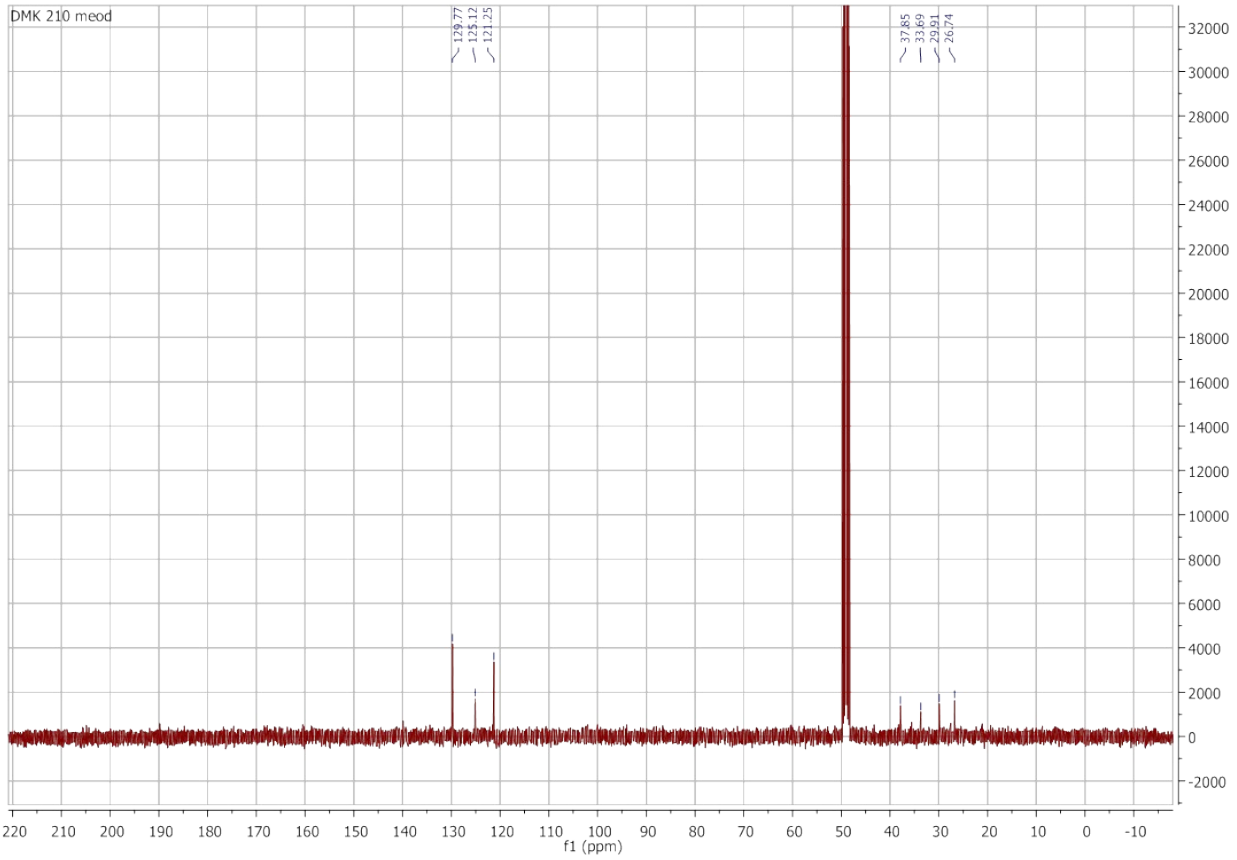

Figure S35. ^{13}C NMR spectrum of [Sb(SAHA$_{-1H}$)(SAHA$_{-2H}$)].

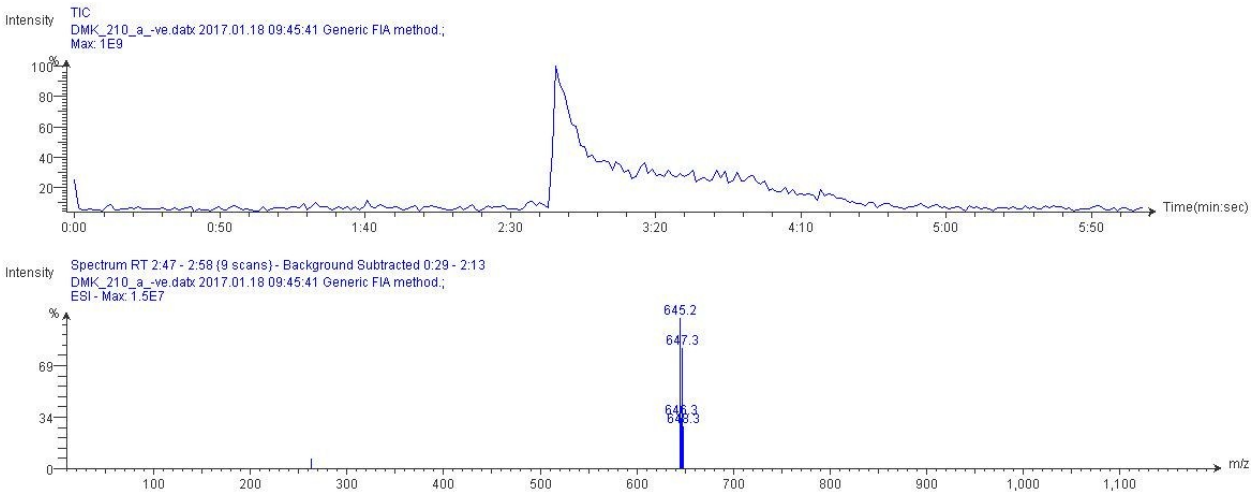

Figure S36. Mass spectrum of [Sb(SAHA$_{-1H}$)(SAHA$_{-2H}$)].

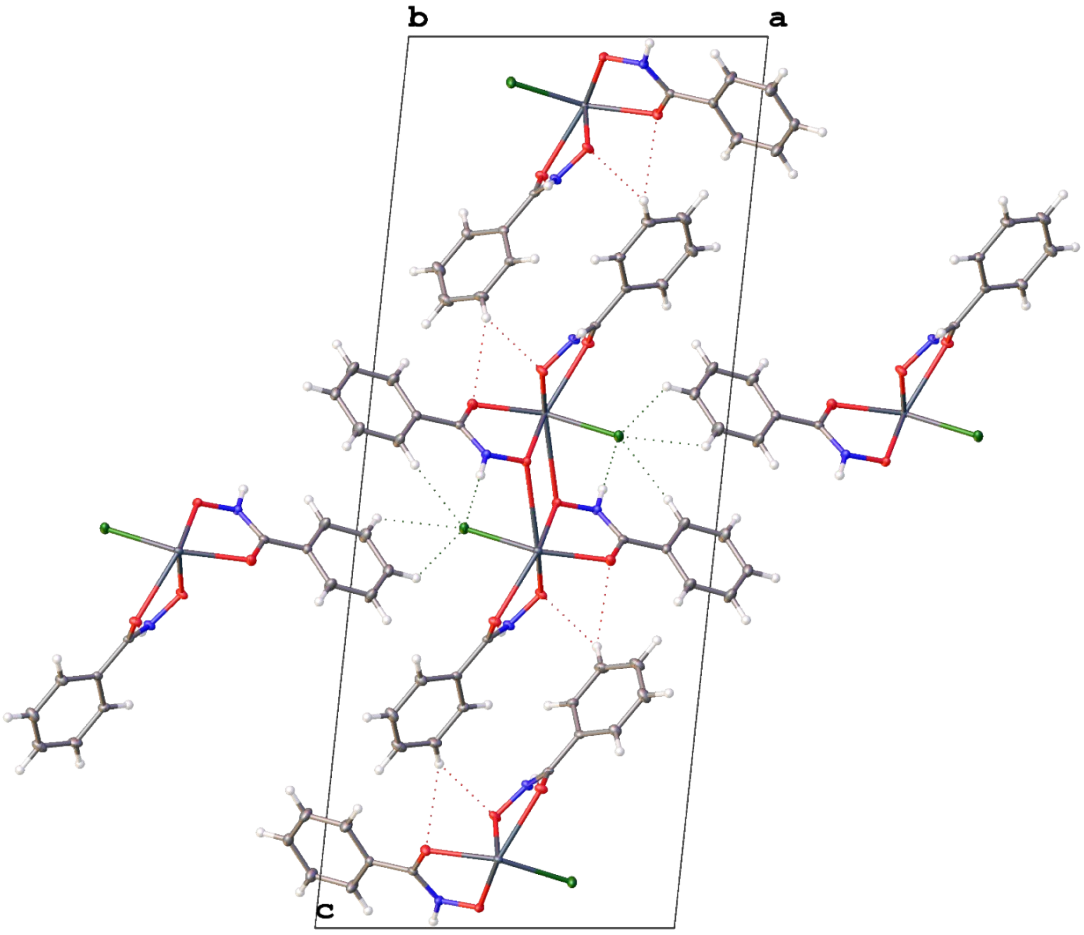

Figure S37. Packing diagram of dimeric **1** viewed normal to the b-axis showing the hydrogen bonding network. Atomic displacement shown at 50% probability.

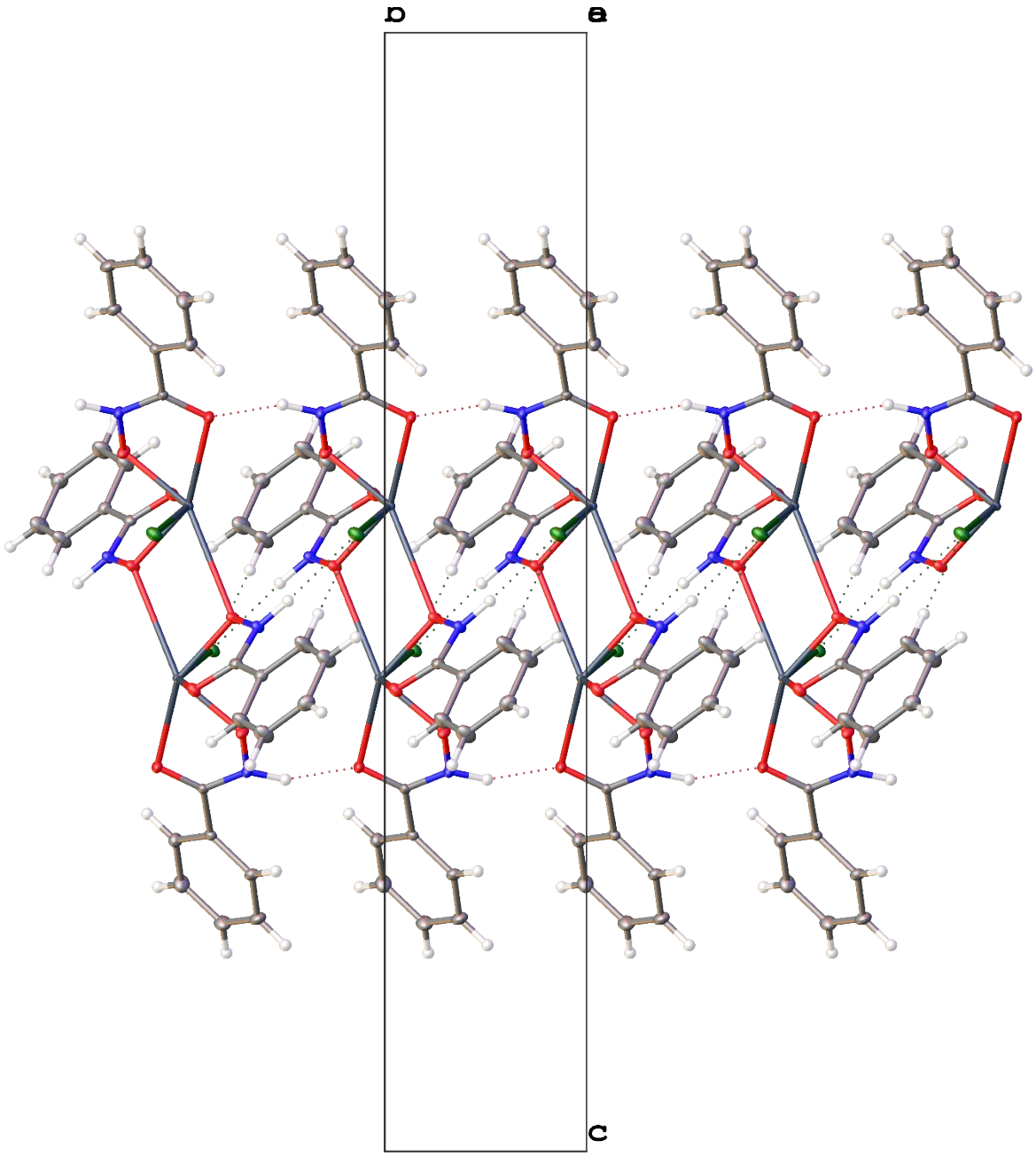

Figure S38. Hydrogen bonding pattern for **1** viewed normal to the a-axis.

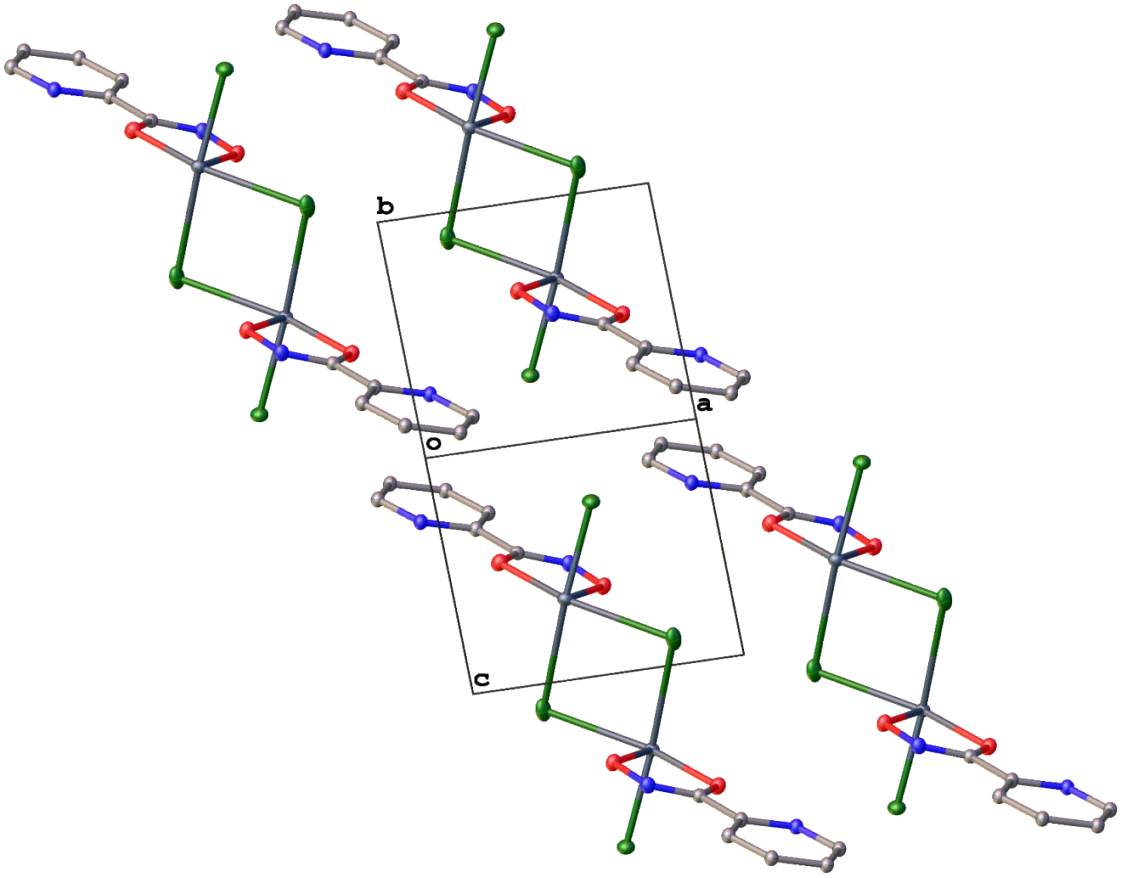

Figure S39. Packing diagram of the major disordered moiety of **2** showing the dimers as viewed normal to (011). Atomic displacement shown at 50% probability. Hydrogen atoms omitted for clarity.

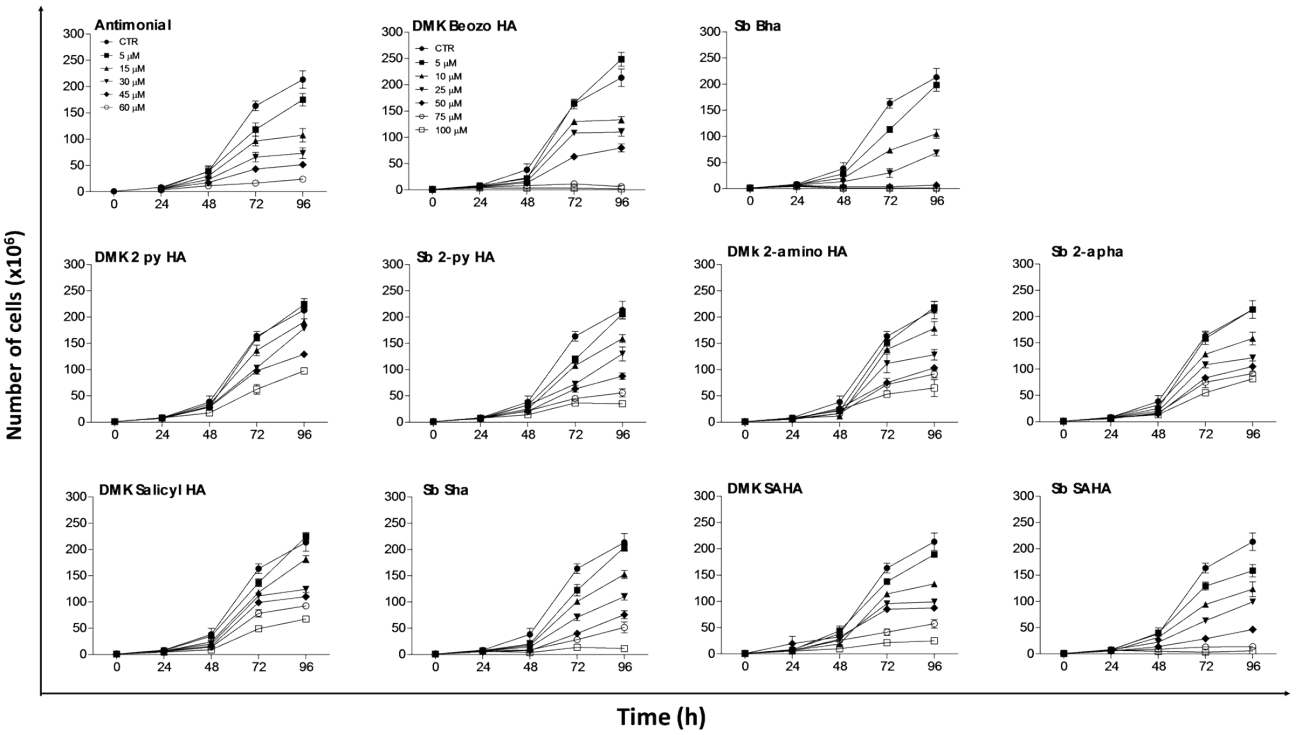

Figure S40: Effects of compounds on the proliferative rate of *L. amazonensis* promastigotes. The proliferation of promastigotes was followed at 28°C in the absence (control) or in the presence of the different concentrations of the compounds for 96 h. The compounds were tested in concentrations ranging from 5 to 100 µM, and antimonial was assayed in concentrations ranging from 5 to 60 µM. Each inhibitor was added to the cultures at 0 h, and viable cells were counted daily by Trypan blue exclusion and mobility in a Neubauer chamber. Data shown are the mean ± standard deviation of three independent experiments performed in triplicate.

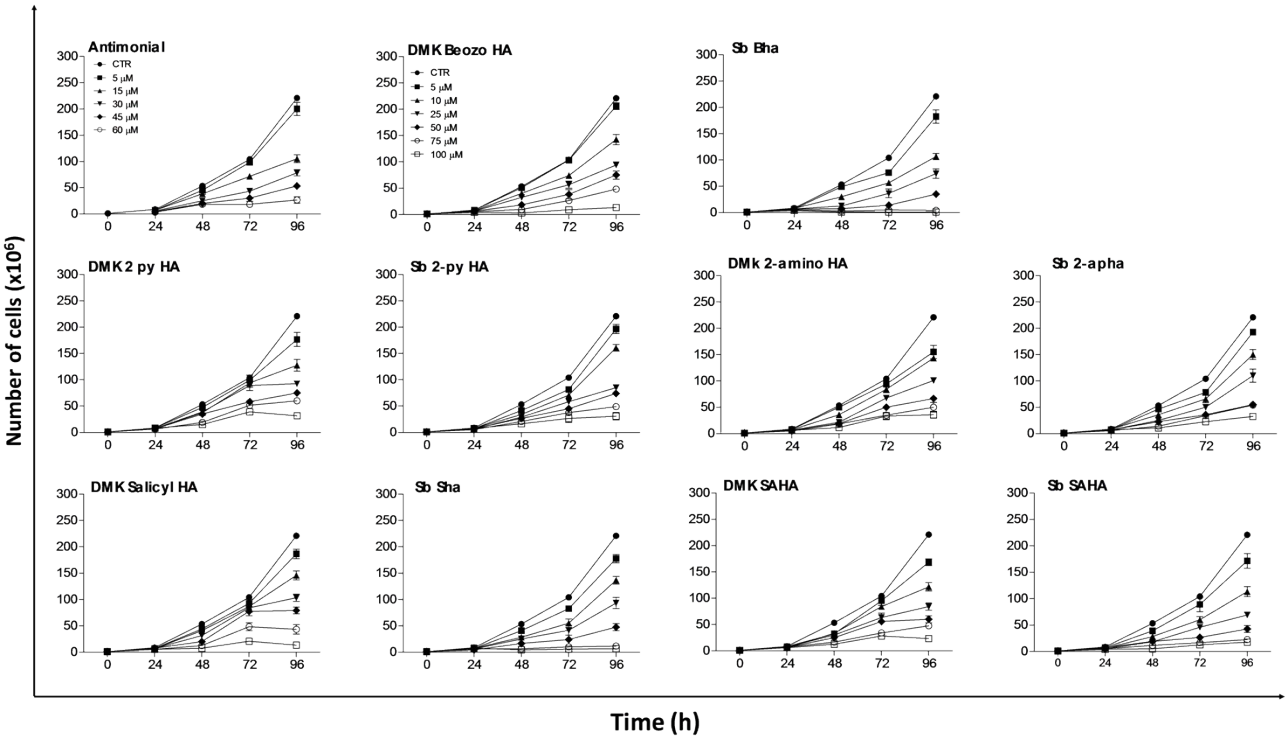

Figure S41. Effects of compounds on the proliferative rate of *L. chagasi* promastigotes. The proliferation of promastigotes was followed at 28°C in the absence (control) or in the presence of the different concentrations of the compounds for 96 h. The compounds were tested in concentrations ranging from 5 to 100 µM, and antimonial was assayed in concentrations ranging from 5 to 60 µM. Each inhibitor was added to the cultures at 0 h, and viable cells were counted daily by Trypan blue exclusion and mobility in a Neubauer chamber. Data shown are the mean ± standard deviation of three independent experiments performed in triplicate.

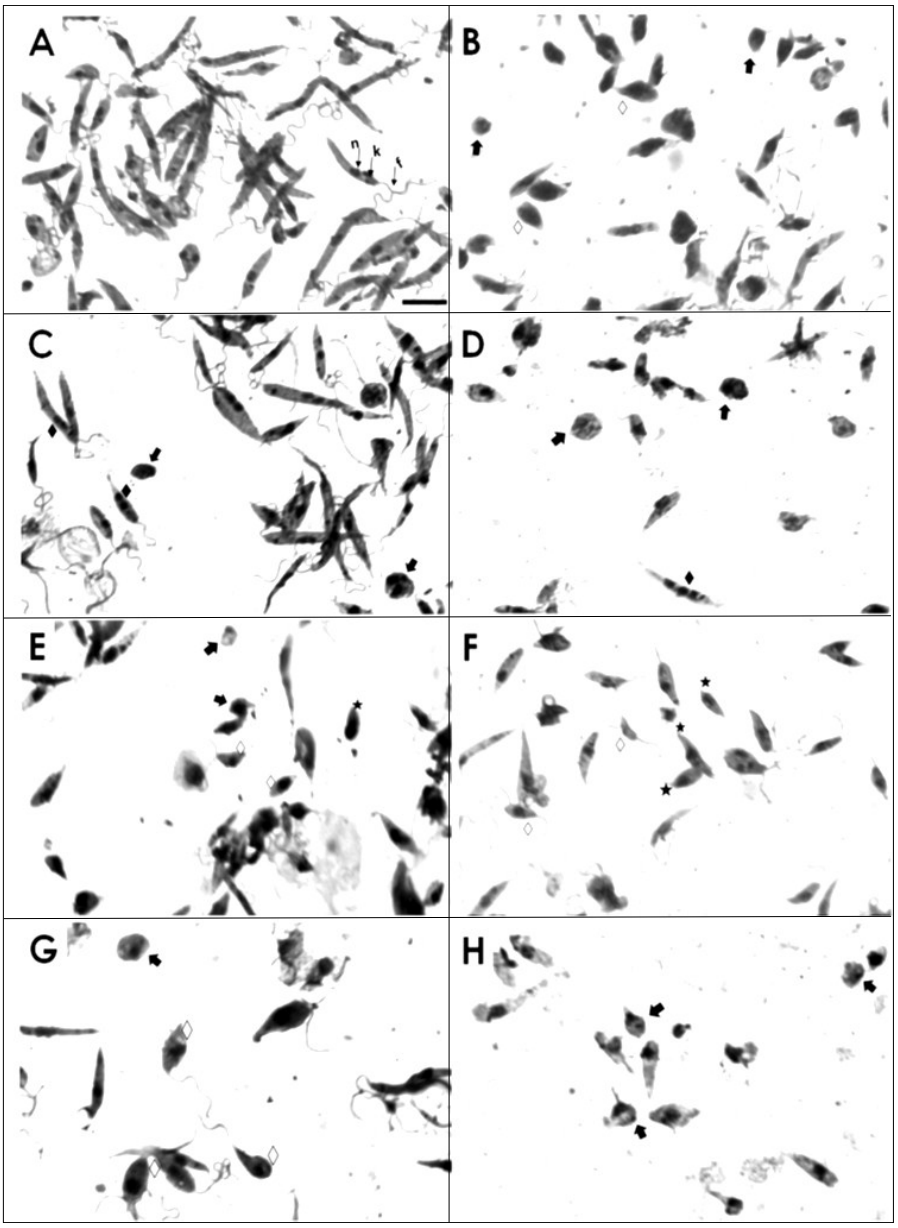

Figure S42: Effects of compounds on morphology of *L. chagasi* promastigotes. Parasites were incubated in the absence (control) (A) or in the presence of IC_{50} value of antimony ((B), Bha (C), **1** (D), 2-NH_2-pha (E), **3** (F), SAHA (G), **6** (H) for 72 h and Giemsa-stained. Untreated forms present a central nucleus (n), kinetoplast (k) in the anterior end of the parasite, an elongated cell body and a flagellum (f) attached to the parasite cell body. Treated promastigotes presented changes such as: rounding (black arrow) or shortening of the cell body (white diamond), increased number of nucleus (black diamond), duplication (asterisk) or absence (black star) of flagellum, presence of cytoplasmic granules (white arrow) and formation of cell clusters (white star). Bars = 10 μM.

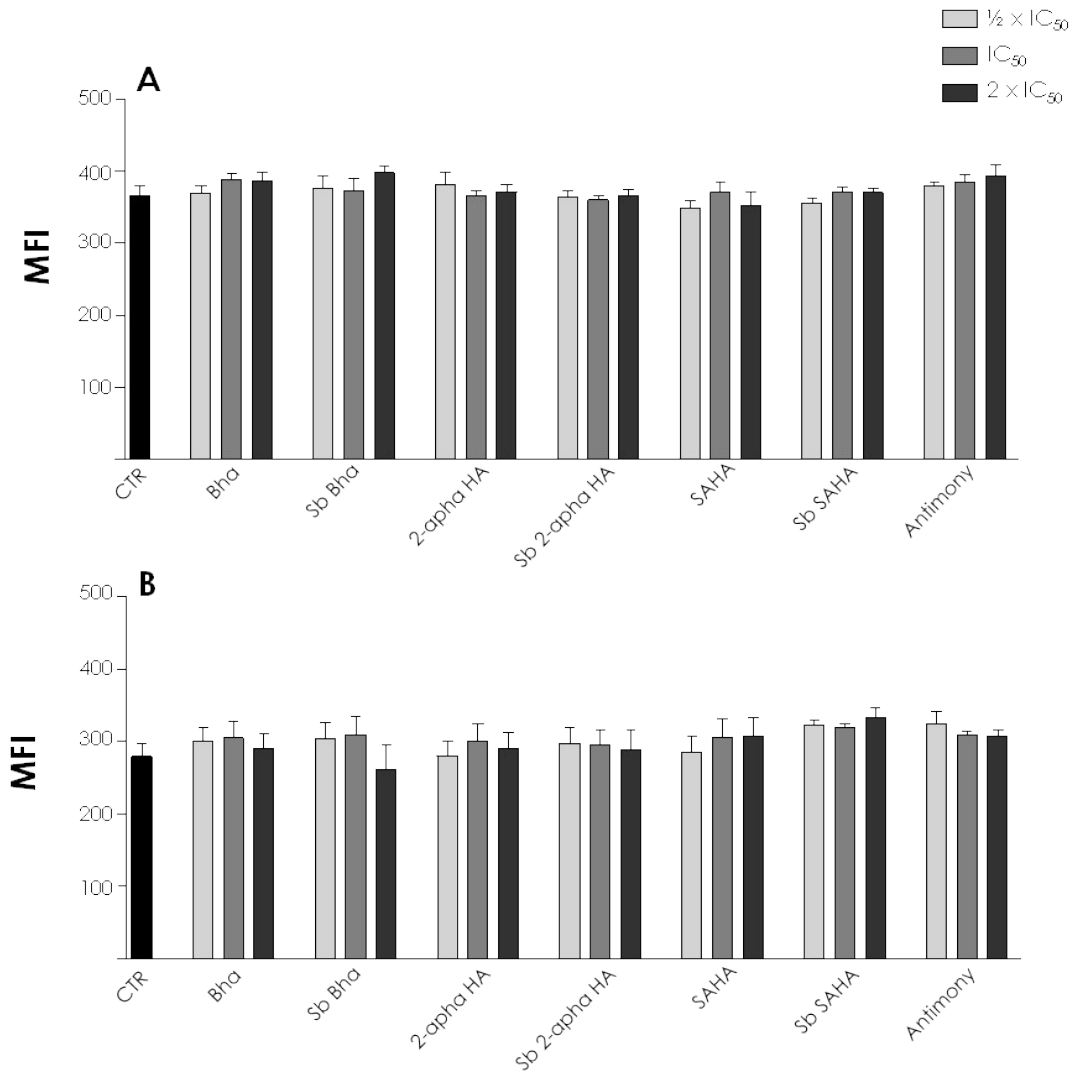

Figure S43. Promastigote forms of *L. amazonensis* (A) and *L. chagasi* (B) were incubated in the absence or presence of ½ x IC_{50}, IC_{50} and 2 x IC_{50} of compounds for 72 and analyzed by flow cytometry in order to evaluate the cell granularity (SSC) of the cells. The data represent the mean and standard deviation (SD) of three independent experiments performed in triplicate.